

Distributed User Scheduling for MIMO-Y Channel

Hui Gao, *Member, IEEE*, Chau Yuen, *Senior*

Member, IEEE, Yuan Ren, Wei Long, Tiejun Lv, *Senior Member, IEEE*

Abstract

In this paper, distributed user scheduling schemes are proposed for the multi-user MIMO-Y channel, where three N_T -antenna users ($N_T = 2N, 3N$) are selected from three clusters to exchange information via an N_R -antenna amplify-and-forward (AF) relay ($N_R = 3N$), and $N \geq 1$ represents the number of data stream(s) of each unicast transmission within the MIMO-Y channel. The proposed schemes effectively harvest multi-user diversity (MuD) without the need of global channel state information (CSI) or centralized computations. In particular, a novel reference signal space (RSS) is proposed to enable the distributed scheduling for both cluster-wise (CS) and group-wise (GS) patterns. The minimum user-antenna (Min-UA) transmission with $N_T = 2N$ is first considered. Next, we consider an equal number of relay and user antenna (ER-UA) transmission with $N_T = 3N$, with the aim of reducing CSI overhead as compared to Min-UA. For ER-UA transmission, the achievable MuD orders of the proposed distributed scheduling schemes are analytically derived, which proves the superiority and optimality of the proposed RSS-based distributed scheduling. These results reveal some fundamental behaviors of MuD and the performance-complexity tradeoff of user scheduling schemes in the MIMO-Y channel.

Index Terms

Multi-user scheduling, MIMO-Y channel, Analog network coding, Multi-way relay, Multi-user diversity.

H. Gao, R. Yuan, W. Long and T. Lv are with the School of Information and Communication Engineering, Beijing University of Posts and Telecommunications, Beijing, 100876, China (e-mail: huigao@bupt.edu.cn, renyuan@bupt.edu.cn, longwei@bupt.edu.cn, lvtiejun@bupt.edu.cn).

C. Yuen are with Singapore University of Technology and Design, Singapore, 138682. (e-mail: yuenchau@sutd.edu.sg).

I. INTRODUCTION

The multi-way relay channel [1] has been considered as a fundamental building block for future cooperative communications. The capacity and degrees-of-freedom of multi-way relay channel have been partially studied by [2]–[4] assuming specific system configurations and traffic patterns. The more general multi-group multi-way relay scenario is considered in [5] with a novel/efficient joint spatial and temporal signal processing. Currently, two basic representatives of the multi-way relay channel have been focused. The first one is the two-way relay channel (TWRC), which has been extensively studied with various wireless network coding (WNC) techniques [6]–[8]. Recent information-theoretic studies on TWRC can be found in [9], [10] and references therein. In particular, the capacity region of TWRC is characterized in [9] with the deterministic approach, then the linear shift deterministic model is employed in [10] to analyze the capacity region of the multi-pair TWRC. The second representative is the MIMO-Y channel [11], which is a novel extension of the TWRC with multiple independent unicast transmissions among three users. As compared to the TWRC, the MIMO-Y channel requires more sophisticated signal processing with WNC and spatial-resource management. Specifically, the basic MIMO-Y channel has been proposed with a new concept of signal space alignment (SSA) [11], which is a novel application of the principle of interference alignment [12]. SSA aligns the bi-directional information from two users at the relay to maximize the utility of the relay antenna, and it also enables the WNC [6], [7] for efficient transmission with the half-duplex relay. Because of its fundamental role and novel transmission schemes, the MIMO-Y channel is now attracting increasing attentions.

The MIMO-Y channel can find many interesting applications in various three-party communication scenarios. For example, in ad-hoc networks, three geographically isolated nodes can exchange messages with the help of the relay; in cellular networks, a group of three users can share information via the relay with flexible cooperative or device-to-device communication protocols; in satellite communication, the satellite often serves as a relay to enable information exchanges among three earth stations. Inspired by the wide range of potential applications, many efforts have been devoted to understanding the fundamental limit of MIMO-Y channel. For example, the achievable degrees-of-freedom and capacity of the MIMO-Y channel have been studied with various antenna configurations at the users or relay [11], [13]–[17]. Specifically,

the original SSA scheme in [11] has been extended to the generalized K -user MIMO-Y channel in [13]. For the single antenna Gaussian Y-channel, the approximate sum-capacity and the capacity region are characterized in [14] and [15] separately. Recently, an asymmetric signal space alignment scheme is proposed in [16] to assist the information exchange of single antenna users and the achievable degrees-of-freedom of four-user MIMO-Y channel is investigated in [17]. Beyond the concerns of the fundamental limit, some practical schemes have been also proposed to enhance the transmission reliability of MIMO-Y channel in the wireless fading environment [18]–[20]. Of particular interests are the diversity-achieving beamforming schemes, which employ extra antennas at the user, i.e., more antennas than the minimum requirement of SSA operation, to perform selective or iterative beamforming optimization [18], [19]. Although these schemes show significant performance improvements as compared to the proof-of-concept scheme in [11], solely relying on the user's redundant antennas for a scalable diversity gain is not always practical. The limited size and power supply of the user's equipment are practical constraints. Therefore, other diversity-achieving schemes are also demanded to complement these beamforming techniques.

Multi-user diversity (MuD), which is known as an important source to combat wireless fading [21], [22], can be potentially exploited for the MIMO-Y channel. It has been noted that although the number of antennas is limited for each user's equipment, a system potentially has multiple users requiring data transmission. Therefore, by carefully scheduling the users' transmissions, significant performance gain can be obtained. The multi-user scheduling has been studied for the traditional broadcasting [23] and multi-user interference channels [24], [25]. Regarding the general multi-way relay channel, the comprehensive solution of user scheduling is still open. Some initial researches have been done for the TWRC with a variety of system configurations [26]–[31], and they offer valuable insights to inspire new applications. However, the designs of efficient user scheduling schemes for the MIMO-Y channel have different challenges than the TWRC. In general, the MIMO-Y channel calls for new user scheduling methods for its unique system and traffic configurations, i.e., each user has multiple antennas to support two independent unicast information flows [11]. In particular, the unique SSA-oriented MIMO-Y transmission requires more sophisticated transmit/receive beamforming designs [11], which are often coupled with the multi-user scheduling metrics [32]. Such coupling may significantly increase the system overheads for CSI and the computation complexity of the scheduling center.

Taking the scheduling methods [23], [26]–[32] for example, they are all conducted in a centralized fashion with global CSI and require relatively complicated computations at the scheduling center. In fact, even in the cellular network with high user density, asking the base station to learn the global CSI is costly [22]. For the MIMO-Y channel, which often fits into the low-complexity and structure-less networks, the assumption of a powerful dedicated scheduling center is not always feasible, especially when one node or user just serves as the immediate relay. Therefore, novel cost-effective scheduling methods are needed for the MIMO-Y channel. As an initial study on this issue, a distributed scheduling scheme with sketchy performance analysis is reported in [33].

In this paper, we consider a basic multi-user MIMO-Y channel, where one N_R -antenna relay ($N_R = 3N$) helps information exchange among three selected N_T -antenna ($N_T = 2N, 3N$) users from three clusters, and $N \geq 1$ represents the number of data stream(s) of each unicast transmission within the MIMO-Y channel. Such basic configuration is sufficient to capture the essential of the MIMO-Y transmission; it also simplifies MuD analysis for clear insight. In particular, we propose low-complexity distributed user scheduling schemes for the MIMO-Y channel with two scheduling patterns, namely, cluster-wise scheduling (CS) and group-wise scheduling (GS). For the CS, a cluster representative is selected from each cluster, and the three selected representatives conduct information exchange via the relay. Such scheduling may find applications in the wireless ad-hoc or sensor networks. For example, when some globally critical events are observed by many on-site nodes at three isolated places, one node is selected from each cluster to perform information exchange. For the GS, three users (each from a different cluster) are associated within a predefined group before transmission, and one group is scheduled to exchange information via the relay. Such scheduling may be useful in the cellular networks or device-to-device networks where a group of three users wishes to share information within their social network.

Moreover, depending on the number of required antennas equipped at the user, two possible MIMO-Y transmission schemes are considered. Specifically, the transmission scheme with the *minimum* number of *user antenna* (Min-UA) $N_T = 2N$ is first considered with a variable-gain AF relay. It is noted that after user scheduling the Min-UA transmission adopts a joint beamforming to achieve SSA at the relay, where the three selected users and the relay need to know the three-party CSI. Aiming at reducing CSI overhead, the user antenna is increased as $N_T = 3N$,

and the transmission with an *equal* number of *relay* and *user antenna* (ER-UA) is proposed with a fixed-gain AF relay. The ER-UA transmission allows distributed beamforming at the user with local CSI, which reduces the CSI overhead. In contrast to the centralized scheduling schemes [23], [26]–[32], the proposed schemes can distribute the computations of scheduling metrics to the users with local CSI. Therefore, the scheduling center enjoys very low implementation complexity without global CSI.

The objective of this paper is to study low-complexity distributed CS and GS for MIMO-Y channel with both Min-UA and ER-UA transmissions. Specifically, the key contributions are summarized as follows.

1) A novel reference signal space (RSS) is proposed to guide the distributed scheduling with both Min-UA and ER-UA transmissions. The RSS is a predefined signal space which is known to all the nodes in the network. Under the guidance of RSS, each user can calculate its individual scheduling metric with local CSI, which enables several distributed scheduling schemes with global benefits.

2) RSS-based distributed CS and GS are proposed for Min-UA transmission. Noting that the optimal CS and GS are not decomposable for distributed implementations with Min-UA transmission [32], two sub-optimal angle-based scheduling strategies are proposed with RSS, which enable distributed implementations of CS and GS. Specifically, each user can calculate its angle/chordal-distance coordinate within the RSS by using only local CSI, and the coordinate is used to infer the relative positions of the pair-wisely aligned signal vectors/spaces within the SSA-resultant signal space at the relay. It is interesting to note that the selected users can generate a near-orthogonal SSA-resultant signal space at the relay when $N = 1$ and can better shape the SSA-resultant signal space when $N > 1$, which results in improved system performance.

3) RSS-based distributed CS and GS are proposed for ER-UA transmission. Aiming at utilizing only local CSI, RSS is used to guide both distributed beamforming and scheduling with ER-UA transmission. In particular, each user can calculate its beamforming matrix as well as the individual scheduling metric with local CSI and RSS. It is noted that the locally calculated individual scheduling metric is equivalent to the link gain of MIMO-Y channel. Therefore, such individual metric has a straightforward connection to the optimal (centralized) scheduling metric that is a function of all the link gains. By using the local and individual scheduling metric, effective distributed scheduling schemes are shown to achieve near-optimal performances.

4) The performances of the proposed schemes are analyzed. Specifically, RSS-based distributed CS and GS are carefully analyzed for ER-UA transmission, because of their near-optimal performances and tractability. It is interesting to note that the distributed scheduling achieves the same MuD order as the centralized scheduling under ER-UA transmission. This observation is theoretically proved by studying the network's outage probabilities and the achievable diversity-multiplexing tradeoffs (DMTs) [34] with both centralized and distributed scheduling schemes. The explicit MuD orders are obtained as $d_{CS}^* = \min(M_1, M_2, M_3)$ for both distributed and centralized CS, and $d_{GS}^* = M$ for both distributed and centralized GS, where M_k is the number of candidates in the k -th cluster $k \in \{1, 2, 3\}$, and M is the number of candidate groups. Considering the former works in [32], [33], these results not only prove the optimality of the proposed distributed scheduling in terms of MuD order, but also shed light into the MuD behaviors in MIMO-Y channel.

Organization: Section II introduces the system model and the general MIMO-Y transmission. Section III describes the distributed CS and GS with Min-UA transmission. Section III details the ER-UA transmission and the corresponding distributed CS and GS, and Section IV analyzes the outage probabilities and the achievable DMTs. Numerical results and brief complexity analysis are summarized in Section VI, and Section VII concludes this paper.

Notations: The integer set $\{1, 2, \dots, K\}$ is abbreviated as $[1, K]$. $[\mathbf{A}]_{m,n}$, $(\mathbf{A})^*$, $(\mathbf{A})^T$, $(\mathbf{A})^H$, $(\mathbf{A})^{-1}$, $\text{Tr}(\mathbf{A})$, $\text{vec}(\mathbf{A})$, $\text{Range}(\mathbf{A})$, $\lambda_{\min}(\mathbf{A})$ and $\|\mathbf{A}\|_F$ are the (m, n) -th entry, conjugate, transpose, conjugate transpose, inverse, trace, vectorization, range, minimum eigenvalue and F -norm of a matrix \mathbf{A} . $\mathbf{I}_{m \times m}$ and $\mathbf{0}_{m \times m}$ represent the $m \times m$ identity matrix and all-zero matrix. $\text{Span}(\mathbf{a}, \mathbf{b})$ denotes the subspace spanned by vectors \mathbf{a} and \mathbf{b} , $\|\mathbf{a}\|$ and $\langle \mathbf{a} \rangle = \mathbf{a} / \|\mathbf{a}\|$ are the Euclidean-norm and the normalization operation of vector \mathbf{a} . $\angle(\mathbf{a}, \mathbf{b}) = \cos^{-1} \left(\frac{|\mathbf{a}^H \mathbf{b}|}{\|\mathbf{a}\| \|\mathbf{b}\|} \right)$ is the acute angle between vector \mathbf{a} and \mathbf{b} . \mathbb{C} represents the set of complex numbers. $\mathcal{CN}(\mathbf{m}, \mathbf{\Sigma})$ denotes a complex Gaussian random vector with mean \mathbf{m} and covariance matrix $\mathbf{\Sigma}$. $\mathbb{E}\{\cdot\}$ is the expectation operator. $\binom{n}{k}$ is the number of k -combinations from a given set of n elements. \doteq is the exponential equality, e.g., $f(x) \doteq x^a$ represents $a = \lim_{x \rightarrow \infty} \frac{\log(f(x))}{\log(x)}$.

II. SYSTEM MODEL AND MIMO-Y TRANSMISSION

As shown in Fig. 1, a MIMO-Y network comprises an N_R -antenna relay R and three clusters of N_T -antenna users $\left\{ \mathcal{S}_{j_k(k)}, j_k \in [1, M_k], k \in [1, 3] \right\}$, j_k and M_k are the intra-cluster user index

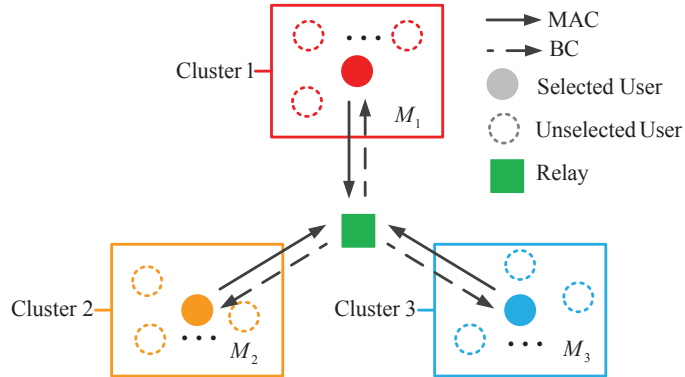


Fig. 1. User scheduling for MIMO-Y channel, where one user is selected from each cluster to exchange information via a relay. The ANC-based protocol is used which consists of MAC and BC phases.

and the number of candidates within the k -th cluster. It is noted that $S_{j_k(k)}$ contains two subscripts, namely j_k and k ; for notational simplicity, we may omit the second subscript k for most of the scenarios, if not causing confusing¹. It is assumed that there is no direct link between any two users in different clusters, and the half-duplex AF relay helps information exchange among clusters. Time-division duplex (TDD) mode is assumed, therefore channel reciprocity holds. The channels of $S_{j_k} \rightarrow R$ and $R \rightarrow S_{j_k}$ are denoted as $\mathbf{H}_{j_k} \in \mathbb{C}^{N_R \times N_T}$ and $\mathbf{H}_{j_k}^T \in \mathbb{C}^{N_T \times N_R}$, respectively, whose entries are independent and identically distributed (i.i.d.) $\mathcal{CN}(0, 1)$. User scheduling is the focus of this paper, and only one user is selected from each cluster. The three selected users then exchange information through the basic MIMO-Y channel [11]. More specifically, each user sends two unicast messages for the other two users, and intends to decode two messages from the other users. Before presenting the specific transmission and scheduling schemes, the outline of the general MIMO-Y transmission is reviewed in this section. For the ease of exposition, the intra-cluster index of each user is temporarily neglected, and the selected user in the k -th cluster is denoted as S_k . Accordingly, the relevant channels of S_k are denoted as \mathbf{H}_k and \mathbf{H}_k^T , respectively. In addition, the information symbols from S_k to another two users $\{S_l\}_{l \in \mathcal{L}_k}$ are collected in $\{\mathbf{d}_{l,k}\}_{l \in \mathcal{L}_k}$, $\mathcal{L}_k = [1, 3] \setminus \{k\}$, where $\mathbf{d}_{l,k} = [d_{l,k}^{[1]}, d_{l,k}^{[2]}, \dots, d_{l,k}^{[N]}]^T \in \mathbb{C}^{N \times 1}$ is the unicast of $S_k \rightarrow S_l$ containing N data streams. Analog network coding (ANC) [6] is employed for efficient AF relaying, which consists of the multiple access (MAC) and broadcasting (BC)

¹If we do not want to specify a user, we can understand S_{j_k} as the j_k -th user of the k -th cluster, even if we omit the second subscript k . If we want to specify, for example, the 2nd user in the 1st cluster, we reminder the two subscripts and denote it as S_{2_1} . Therefore, the single subscript j_k may indicate an omitted subscript k .

transmission phases. In the MAC phase, ANC treats the superimposed signals as network-coded symbols and just amplify-and-forwards them in the BC phase. Upon receiving the broadcasted symbols from the relay, users extract the desired signals by virtue of self-interference cancelation. In order to exploit ANC for MIMO-Y transmission, during the MAC phase, user S_k uses the transmit beamforming matrix $\mathbf{V}_k = [\mathbf{V}_{l_1,k} \ \mathbf{V}_{l_2,k}] \in \mathbb{C}^{N_T \times 2N}$ for data, and the transmitted symbol vector is $\mathbf{s}_k = \mathbf{V}_k \mathbf{d}_k \in \mathbb{C}^{N_T \times 1}$, where $\mathbf{d}_k = [\mathbf{d}_{l_1,k}^T \ \mathbf{d}_{l_2,k}^T]^T \in \mathbb{C}^{2N \times 1}$ and $\mathbb{E}\{\mathbf{d}_k \mathbf{d}_k^H\} = \mathbf{I}_{2N \times 2N}$, $k \in [1, 3]$, $l_1, l_2 \in \mathcal{L}_k$, $l_1 \neq l_2$. A transmit power constraint is imposed as $\text{Tr}(\mathbf{V}_k \mathbf{V}_k^H) \leq P_T$, where P_T is the average transmit power of each user. Then, the relay R receives

$$\mathbf{y}_R = \sum_{k=1}^3 \mathbf{H}_k \mathbf{s}_k + \mathbf{n}_R, \quad (1)$$

where $\mathbf{n}_R \in \mathbb{C}^{N_R \times 1} \sim \mathcal{CN}(\mathbf{0}, \sigma_R^2 \mathbf{I}_{N_R \times N_R})$ is the additive white Gaussian noise (AWGN) vector. During the BC phase, the transmitted signal of the AF relay is given as² $(\mathbf{s}_R)^* = (\mathbf{W} \mathbf{y}_R)^* = (G_R \tilde{\mathbf{W}} \mathbf{y}_R)^* \in \mathbb{C}^{N_T \times 1}$, where $\tilde{\mathbf{W}} \in \mathbb{C}^{N_R \times N_R}$ is the relay processing matrix and G_R is the power controlling coefficient to be specified later. Then, the conjugated received signal at S_k is expressed as

$$\mathbf{y}_k = (\tilde{\mathbf{y}}_k)^* = (\mathbf{H}_k^T (\mathbf{s}_R)^* + \tilde{\mathbf{n}}_k)^* = \mathbf{H}_k^H \mathbf{s}_R + \mathbf{n}_k \quad (2)$$

where $\tilde{\mathbf{y}}_k = \mathbf{H}_k^T (\mathbf{s}_R)^* + \tilde{\mathbf{n}}_k$ is the received signal before conjugating, $\tilde{\mathbf{n}}_k, \mathbf{n}_k \in \mathbb{C}^{N_T \times 1}$ is the AWGN vector distributed as $\mathcal{CN}(\mathbf{0}, \sigma_S^2 \mathbf{I}_{N_T \times N_T})$. According to the ANC protocol, S_k needs to perform self-interference cancellation before extracting the useful information sent by $\{\mathbf{S}_l\}_{l \in \mathcal{L}_k}$ with the receive beamforming matrix $\mathbf{U}_k \in \mathbb{C}^{N_T \times 2N}$, which is described as

$$\hat{\mathbf{y}}_k = \mathbf{U}_k^H (\mathbf{y}_k - \mathbf{H}_k^H \mathbf{W} \mathbf{H}_k \mathbf{s}_k) = \hat{\mathbf{y}}_{k,S} + \hat{\mathbf{y}}_{k,\sigma}, \quad (3)$$

where $\hat{\mathbf{y}}_{k,S} = \mathbf{U}_k^H \mathbf{H}_k^H \mathbf{W} \sum_{l \in \mathcal{L}_k} \mathbf{H}_l \mathbf{V}_l \mathbf{d}_l \in \mathbb{C}^{N_T \times 1}$ and $\hat{\mathbf{y}}_{k,\sigma} = \mathbf{U}_k^H (\mathbf{H}_k^H \mathbf{W} \mathbf{n}_R + \mathbf{n}_k) \in \mathbb{C}^{N_T \times 1}$ are the signal component and the noise component of the decision variable $\hat{\mathbf{y}}_k$, respectively. With a proper design of transmit/receive beamforming matrices $\{\mathbf{U}_k, \mathbf{V}_k\}_{k=1}^3$ at each user and \mathbf{W} at the relay, S_k can have interference-free reception and recover the useful information as $(\hat{\mathbf{d}}_{k,l_1} \ \hat{\mathbf{d}}_{k,l_2}) = f_k(\hat{\mathbf{y}}_k)$, $l_1, l_2 \in \mathcal{L}_k$, $l_1 \neq l_2$, where f_k represents the decoding process at S_k . In the next sections, we will show the detailed designs of $\{\mathbf{U}_k, \mathbf{V}_k\}_{k=1}^3$ and \mathbf{W} for Min-UA and ER-UA transmissions as well as their corresponding CS and GS. It is also noted that we mainly focus on two typical antenna configurations, namely $\frac{N_R}{N_T} = \frac{3}{2}$ and $\frac{N_R}{N_T} = 1$, and $N_R = 3N$, which represents the Min-UA transmission and the ER-UA transmission, respectively.

²Similar to the treatment in [35], we use conjugate operations at both transmitter and receiver, so that the channel matrix \mathbf{H}_k^T can be in the form of hermitian transpose in (2).

III. DISTRIBUTED USER SCHEDULING WITH MIN-UA TRANSMISSION

In this section, the distributed user scheduling schemes are studied with the Min-UA transmission, where each user is equipped with $N_T = 2N$ antennas and the relay is equipped with $N_R = 3N$ antennas, $N \geq 1$. It is noted that in this scenario the instantaneous three-party CSI is required by the three selected users and the relay for joint beamforming [11]. Because of this coupling, the calculation of the optimal scheduling metric, i.e., the post-processing signal-to-noise-ratio (SNR), cannot be easily decomposed, and the design of an effective distributed user scheduling is very challenging. To this end, a novel RSS is introduced to guide the distributed CS and GS. To be more specific, the RSS is a predefined signal space $\Omega_R = \text{Span} \left(\left\{ \mathbf{e}_I^{[n]}, \mathbf{e}_{II}^{[n]}, \mathbf{e}_{III}^{[n]} \right\}_{n=1}^N \right)$, whose normalized orthogonal basis $\mathbf{E} = [\mathbf{E}_I \mathbf{E}_{II} \mathbf{E}_{III}] \in \mathbb{C}^{N_R \times N_R}$ is assumed to be known by all the users in this network, where $\mathbf{E}_m = [\mathbf{e}_m^{[1]}, \mathbf{e}_m^{[2]}, \dots, \mathbf{e}_m^{[N]}] \in \mathbb{C}^{N_R \times N}$ can span a subspace³, $m \in \{I, II, III\}$. It is noted that, \mathbf{E} can be arbitrary normalized orthogonal basis of the N_R -dimensional space and can be designed off-line or broadcasted by the relay. Before presenting the RSS-based distributed user scheduling schemes, the Min-UA transmission is briefly described in the following subsection.

A. Min-UA Transmission

Without loss of generality, let us assume three users $\{S_1, S_2, S_3\}$ are randomly selected to perform Min-UA MIMO-Y transmission. In the MAC phase, each user sends 2 unicast messages which consists of $2N$ independent data streams. Therefore, there are $6N$ data streams arriving at the relay simultaneously. Since the relay is only equipped with $N_R = 3N$ antennas, it is not able to decode these signals in a stream-by-stream fashion. In order to utilize the relay antennas more efficiently, SSA is introduced into the MIMO Y channel. In particular, SSA is required for the bi-directional information exchange between the pair S_l and S_k , $k \in [1, 3]$, $l \in \mathcal{L}_k$, and the transmit beamforming matrix of each user is jointly designed with another two users using the three-party CSI. More specifically, the pair-wise transmit beamforming matrices of S_l and S_k can be *jointly* designed by solving the null-space problem [11] as

$$[\mathbf{H}_l \quad -\mathbf{H}_k] \tilde{\mathbf{V}}_{m=\pi(l,k)} = \mathbf{0}, \quad (4)$$

³For notational clarity, a permutation function over the source index pair (l, k) is introduced as $m = \pi(l, k) = \pi(k, l)$, $m, k \in [1, 3]$, $l \in \mathcal{L}_k$. Specifically, π is defined as $\pi(1, 2) = I$, $\pi(1, 3) = II$, $\pi(2, 3) = III$.

where $\tilde{\mathbf{V}}_m = \begin{bmatrix} \tilde{\mathbf{V}}_{k,l}^T & \tilde{\mathbf{V}}_{l,k}^T \end{bmatrix}^T \in \mathbb{C}^{2N_T \times N}$ contains the pair-wise transmit beamforming matrices, $\tilde{\mathbf{V}}_{k,l}$ and $\tilde{\mathbf{V}}_{l,k}$, with a total power normalization as $\|\tilde{\mathbf{V}}_m\|_F^2 = 1$. For simplicity, a total power constraint P_T is imposed on this pair-wise transmit beamforming matrices, and the effective transmit beamforming matrix for $\mathbf{d}_{l,k}$ is expressed as

$$\mathbf{V}_{l,k} = \sqrt{P_T} \tilde{\mathbf{V}}_{l,k}. \quad (5)$$

It is easy to check that each unicast message of S_k has an average power of $\mathbb{E} \{ \|\mathbf{V}_{l,k}\|_F^2 \} = \frac{1}{2} P_T$, therefore, the average transmit power of each user is P_T . According to (4) and (5), it is noted that the three-party CSI is necessary for the beamforming matrix $\mathbf{V}_k = [\mathbf{V}_{l_1,k} \ \mathbf{V}_{l_2,k}]$ of S_k , $l_1, l_2 \in \mathcal{L}_k$, $l_1 \neq l_2$. Employing the pair-wise transmit beamforming matrix $\mathbf{V}_{k,l}$ and $\mathbf{V}_{l,k}$, the bi-directional signal between S_l and S_k is then aligned within a N -dimensional subspace spanned by the column vectors of $\mathbf{F}_{m=\pi(k,l)} = \mathbf{H}_l \tilde{\mathbf{V}}_{k,l} = \mathbf{H}_k \tilde{\mathbf{V}}_{l,k} \in \mathbb{C}^{N_R \times N}$, which is within the signal space of \mathbf{R} , and the received signal at \mathbf{R} is given by (cf. (1))

$$\mathbf{y}_R = \sqrt{P_T} \mathbf{F} \mathbf{d}_+ + \mathbf{n}_R, \quad (6)$$

where $\mathbf{F} = [\mathbf{F}_I \ \mathbf{F}_{II} \ \mathbf{F}_{III}] \in \mathbb{C}^{N_R \times N_R}$ is the signal space seen by \mathbf{R} with $\mathbf{F}_m = [\mathbf{f}_m^{[1]}, \mathbf{f}_m^{[2]}, \dots, \mathbf{f}_m^{[N]}] \in \mathbb{C}^{N_R \times N}$, and $\mathbf{d}_+ = [\mathbf{d}_{+,1}^T \ \mathbf{d}_{+,2}^T \ \mathbf{d}_{+,3}^T]^T \in \mathbb{C}^{3N \times 1}$ is the superimposed signal with element $\mathbf{d}_{+,m} = \mathbf{d}_{l,k} + \mathbf{d}_{k,l}$. Taking $N_R = 3$ as an example⁴, Fig. 2 describes the idea of SSA. For simplicity, we follow [18] and use the zero forcing (ZF)-based relay processing matrix $\mathbf{W} = G_R \tilde{\mathbf{W}} = G_R (\mathbf{F}^H)^{-1} \mathbf{F}^{-1} = G_R (\mathbf{F} \mathbf{F}^H)^{-1} \in \mathbb{C}^{N_R \times N_R}$ at \mathbf{R} , where \mathbf{F}^{-1} is the detection matrix and $(\mathbf{F}^H)^{-1}$ is the transmit beamforming matrix. It is noted that $\tilde{\mathbf{W}}$ decouples the equivalent channel matrices of the MAC and BC phases respectively, so that the users can obtain the desired superimposed signals or network-coded signals at low cost. Here, G_R is the power controlling coefficient of the variable-gain AF relay, and it is calculated as

$$G_R = \sqrt{P_R / \mathbb{E} \{ \|\mathbf{x}_R\|^2 \}} = \sqrt{P_R / (P_T \text{Tr}(\tilde{\mathbf{W}}) + \sigma_R^2 \text{Tr}(\tilde{\mathbf{W}} \tilde{\mathbf{W}}^H))}, \quad (7)$$

where $\mathbf{x}_R = \mathbf{W} \mathbf{y}_R = G_R \sqrt{P_T} (\mathbf{F}^H)^{-1} \mathbf{d}_+ + G_R \tilde{\mathbf{W}} \mathbf{n}_R$ is the signal broadcasted by the relay, and the expectation on $\|\mathbf{x}_R\|^2$ is over \mathbf{d}_+ and \mathbf{n}_R .

At each user S_k , the received signal is given by (2), then the remaining signal after subtracting self-interference is given by

$$\tilde{\mathbf{y}}_k = \sqrt{P_T} \mathbf{H}_k^H \mathbf{W} \mathbf{F}_k \mathbf{d}_{+,k} + \mathbf{H}_k^H \mathbf{W} \mathbf{n}_R + \mathbf{n}_k, \quad (8)$$

⁴For the ease of illustration, most of the figures are based on the assumption that $N_R = 3$, accordingly, \mathbf{E} is simplified as $\mathbf{E} = [\mathbf{e}_I, \mathbf{e}_{II}, \mathbf{e}_{III}] \in \mathbb{C}^{3 \times 3}$ and \mathbf{F} is simplified as $\mathbf{F} = [\mathbf{f}_I, \mathbf{f}_{II}, \mathbf{f}_{III}] \in \mathbb{C}^{3 \times 3}$ for these figures.

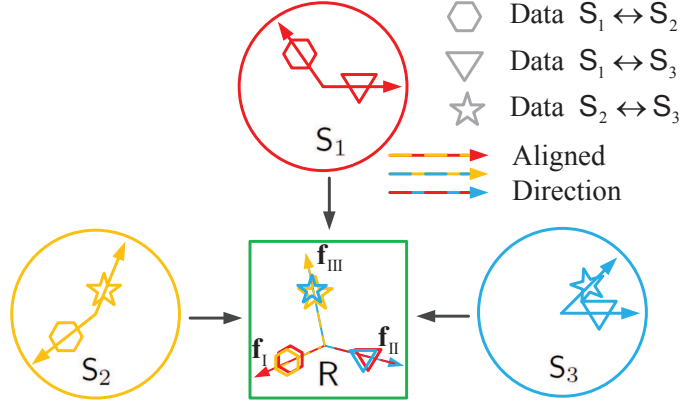


Fig. 2. Geometrical interpretation on the Min-UA transmission. After the joint beamforming, the signals are pair-wisely aligned at the relay during the MAC phase. The aligned directions are not necessarily orthogonal, and the equivalent MIMO channel seen by the relay might be ill-conditioned.

where $\tilde{\mathbf{F}}_k = [\mathbf{F}_{m_1} \mathbf{F}_{m_2} \mathbf{F}_{m'}] \in \mathbb{C}^{N_R \times N_R}$, and $\mathbf{d}_{+,k} = [\mathbf{d}_{k,l_1}^T \mathbf{d}_{k,l_2}^T \mathbf{d}_{+,m'}^T]^T \in \mathbb{C}^{3N \times 1}$, $m_1 = \pi(l_1, k)$, $m_2 = \pi(l_2, k)$, $l_1, l_2 \in \mathcal{L}_k$ and $m' \in [1, 3] \setminus \{m_1, m_2\}$. Then the receive beamforming $\mathbf{U}_k = [\mathbf{U}_{l_1,k} \mathbf{U}_{l_2,k}] = [\mathbf{V}_{l_1,k} \mathbf{V}_{l_2,k}] \in \mathbb{C}^{N_T \times 2N}$ is applied to obtain $\hat{\mathbf{y}}_k = \mathbf{U}_k^H \tilde{\mathbf{y}}_k$. More specifically, $\mathbf{U}_{l,k} = \mathbf{V}_{l,k}$ is used to get the signal from S_l as $\hat{\mathbf{y}}_{k,l} = \mathbf{U}_{l,k}^H \tilde{\mathbf{y}}_k$, and each desired signal stream within $\hat{\mathbf{y}}_{k,l}$ is given by

$$\hat{y}_{k,l}^{[n]} = \sqrt{P_T} G_R d_{k,l}^{[n]} + G_R \mathbf{a}_n^T \mathbf{F}_m^H \tilde{\mathbf{W}} \mathbf{n}_R + \mathbf{a}_n^T \mathbf{V}_{l,k}^H \mathbf{n}_k, \quad n \in [1, N], \quad (9)$$

where the elements of $\mathbf{a}_n \in \mathbb{C}^{N \times 1}$ are all zeros except the n -th element that equals to one, i.e., \mathbf{a}_n is a Cartesian unit vector. After briefing the Min-UA transmission, the corresponding user scheduling schemes are discussed in the next subsection.

B. Problem Formulation and Centralized Scheduling

In this subsection, the optimal CS and GS are formulated with Min-UA transmission, which serves as a preliminary and reference for distributed scheduling. Some necessary notations and performance metrics are first introduced. For ease of description on CS, an ordered set $J = \{j_1, j_2, j_3\}$ is used as a collection of the user indices⁵, $j_k \in [1, M_k]$, $k \in [1, 3]$, and all the possible realizations of J are enumerated⁶ in another ordered set $\mathcal{J} = \{J_q\}_{q=1}^Q$, $Q = M_1 M_2 M_3$.

⁵It is noted that j_k represents the intra-cluster index of a user $S_{j_k(k)}$. When j_k is specified, the order in J can indicate the cluster k . For example, $J = \{3, 2, 1\}$ represents the 3rd, the 2nd and the 1st users from the 1st, 2nd, 3rd clusters, respectively.

⁶We can order by the first, then by the second, and then by the third elements of J . For example, $J_1 = \{1, 1, 1\} \prec J_2 = \{2, 1, 1\} \prec \dots \prec J_q = \{j_1, j_2, j_3\} \prec \dots \prec J_{M_1 M_2 M_3} = \{M_1, M_2, M_3\}$.

In GS, we have $M_1 = M_2 = M_3 = M$. Then, a subset $\mathcal{J}' \subset \mathcal{J}$ is used to facilitate the description for all the possible realizations of $J'_p = \{j'_1, j'_2, j'_3 | j'_1 = j'_2 = j'_3 = p\}$, which is defined as⁷ $\mathcal{J}' = \{J'_p\}_{p=1}^M$. Regarding the system performance metrics, the overall outage probability of the network with arbitrary selected users $\{S_{j_1}, S_{j_2}, S_{j_3}\}$ is defined as

$$P_{out}^{(J)}(\rho_{th}) = \Pr\left(\rho_{min}^{(J)} \leq \rho_{th}\right), \quad (10)$$

where ρ_{th} is the threshold SNR-value for the outage probability and $\rho_{min}^{(J)}$ is the minimum post-processing SNR (min-SNR) of the network with selected users in J . Then, $\rho_{min}^{(J)}$ is defined as

$$\rho_{min}^{(J)} = \min_{k \in [1,3], l \in \mathcal{L}_k, n \in [1,N]} \left(\rho_{j_k, j_l}^{[n]}\right), \quad (11)$$

where $\rho_{j_k, j_l}^{[n]}$ represents the end-to-end post-processing SNR of the n -th data stream of link $S_{j_l} \rightarrow R \rightarrow S_{j_k}$, $l \in \mathcal{L}_k$, and $\rho_{j_k, j_l}^{[n]} = \mathbb{E} \left\{ \left(\sqrt{P_T} G_R d_{k,l}^{[n]} \right)^2 \right\} / \mathbb{E} \left\{ \left(G_R \mathbf{a}_n^T \mathbf{F}_m^H \tilde{\mathbf{W}} \mathbf{n}_R + \mathbf{a}_n^T \mathbf{V}_{l,k}^H \mathbf{n}_k \right)^2 \right\}$ is calculated with reference to (9) as

$$\rho_{j_k, j_l}^{[n]} = \frac{G_R^2 P_T}{G_R^2 \sigma_R^2 \left[\mathbf{F}_m^H \tilde{\mathbf{W}}^{(J)} \left(\tilde{\mathbf{W}}^{(J)} \right)^H \mathbf{F}_m \right]_{n,n} + \sigma_s^2 \left[\mathbf{V}_{j_l, j_k}^H \mathbf{V}_{j_l, j_k} \right]_{n,n}}, \quad (12)$$

where G_R is given by (7). Based on the aforementioned notations, the centralized CS is given by

$$J_C = \{j_1^*, j_2^*, j_3^*\} = \arg \max_{J \in \mathcal{J}} \left(\rho_{min}^{(J)} \right), \quad (13)$$

and the centralized GS is given by

$$J'_C = \{j'_1, j'_2, j'_3\} = \arg \max_{J' \in \mathcal{J}'} \left(\rho_{min}^{(J')} \right). \quad (14)$$

Similar to the scheduling in [32], both centralized CS and GS involve global CSI and high computational complexity at the scheduling center.

C. RSS-based Distributed scheduling with Min-UA for $N = 1$

In this subsection, RSS-based distributed CS and GS are first proposed with Min-UA transmission for $N = 1$. In particular, RSS \mathbf{E} is introduced to guide the distributed user scheduling so that the SSA-resultant signal space \mathbf{F} can be well-shaped with simple user scheduling. More specifically, the ZF-based transceiver $\tilde{\mathbf{W}}$ is employed at R, which involves the orthogonal

⁷It is noted that the index used for GS could have been subsumed under J or simplified with less symbols, however, we keep this seemingly redundant form to unify the descriptions on user scheduling criteria and the subsequential analysis.

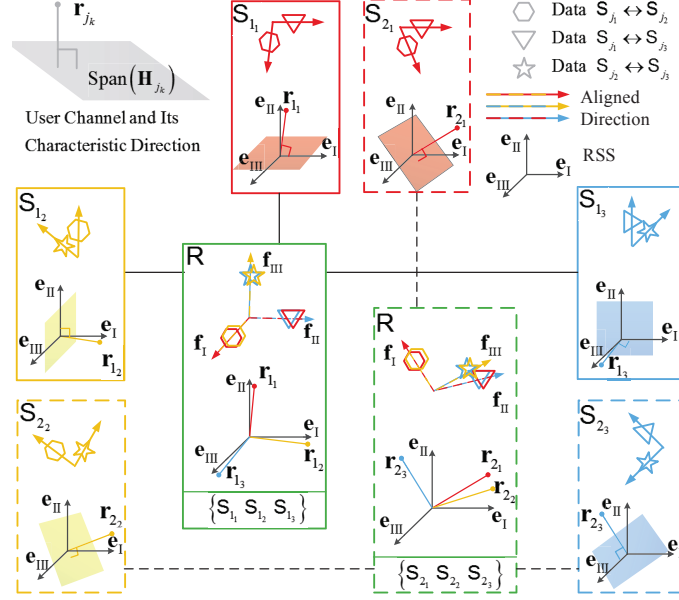


Fig. 3. The geometrical interpretations on the RSS-based distributed user scheduling with Min-UA transmission. In this example, we consider the cluster-wise scheduling and assume that there are two users $\{S_{1_k}, S_{2_k}\}$ in the k -th cluster, $k \in [1, 3]$. The angles between each user's characteristic direction \mathbf{r}_{j_k} and the basis of RSS $\{\mathbf{e}_I, \mathbf{e}_{II}, \mathbf{e}_{III}\}$ can be calculated by the user in a distributed manner. Employing the proposed distributed user scheduling, the pattern of users' characteristic directions can be directly optimized so that the SSA-resultant signal space \mathbf{F} can be indirectly shaped to be more orthogonal.

decomposition and projection on \mathbf{F} and may cause significant power loss especially when \mathbf{F} is ill-conditioned. Intuitively, if one can choose the users to shape \mathbf{F} such that the equivalent channel vectors in \mathbf{F} are almost orthogonal, it is likely that the ZF-resultant power loss can be mitigated and the system performance can be improved.

The interpretations on the orthogonality among channels may have impact on the design of user scheduling. For example, as shown in Fig. 3, a straightforward observation is that we can make $\{\mathbf{f}_m\}_{m=1}^{III}$ near-orthogonal with some particular user scheduling. However, this observation is not instructive for an efficient distributed scheduling with just local CSI. It is noted that \mathbf{f}_m lies in the intersection space of \mathbf{H}_{j_k} and \mathbf{H}_{j_l} , i.e., $\text{Span}(\mathbf{f}_m) = \text{Range}(\mathbf{H}_{j_k}) \cap \text{Range}(\mathbf{H}_{j_l})$, $m = \pi(l, k)$, and the measurement of orthogonality between \mathbf{f}_m and $\mathbf{f}_{m'}$, $m' \neq m$, requires the three-party CSI. Therefore, new methods should be developed to enable distributed scheduling. Considering only local CSI at S_{j_k} , i.e., the channel \mathbf{H}_{j_k} of user S_{j_k} , we first introduce the characteristic direction of the channel as $\mathbf{r}_{j_k} \in \text{Null}(\mathbf{H}_{j_k})$, $\|\mathbf{r}_{j_k}\| = 1$. As shown in Fig. 3, if we

can make $\{\mathbf{r}_{j_k}\}_{k=1}^3$ orthogonal, then the channels $\{\mathbf{H}_{j_k}\}_{k=1}^3$ are pair-wisely perpendicular in the 3-dimensional space, and eventually the intersection spaces of these channels, i.e., $\{\mathbf{f}_m\}_{m=1}^{\text{III}}$, are orthogonal. It is interesting to note that the shaping of $\{\mathbf{f}_m\}_{m=1}^{\text{III}}$ can be achieved in a distributed manner with RSS and local CSI. To make this intuitive observation more concrete, the RSS-based distributed CS and GS are detailed in the following subsections.

1) *RSS-based distributed CS*: Recall that the RSS is a predefined 3-dimensional signal space $\Omega_R = \text{Span}(\mathbf{e}_I, \mathbf{e}_{\text{II}}, \mathbf{e}_{\text{III}})$, which is known by all the users in the network. Then, each user can calculate the angular-coordinate of its characteristic direction within RSS with only local CSI as $\phi_{j_k} = [\phi_{j_k, \text{I}}, \phi_{j_k, \text{II}}, \phi_{j_k, \text{III}}]$, where $\phi_{j_k, m} = \angle(\mathbf{r}_{j_k}, \mathbf{e}_m)$. The proposed RSS-based distributed CS aims to find the best user from each cluster based on the angular-coordinate. Specifically, the RSS-based distributed CS is a three-round sequential scheduling scheme. Let $\mathcal{K}(m) \subseteq [1, 3]$ be the set of candidate cluster-indices for the m -th round, $m \in \{\text{I}, \text{II}, \text{III}\}$. Then, the procedure of distributed CS with Min-UA transmission is summarized as follows:

- 1) Initialization: Let $\mathcal{K}(1) = [1, 3]$.
- 2) User selection: During the m -th round, the user whose characteristic direction is mostly aligned with \mathbf{e}_m is selected from the $\{k \in \mathcal{K}(m)\}$ cluster(s) as

$$j_{\mu(m)}^\dagger = \arg \min_{\{j_k | j_k \in [1, M_k], k \in \mathcal{K}(m)\}} (\phi_{j_k, m}), \quad (15)$$

where $\mu(m)$ represents the cluster-index of the selected user during the m -th round.

- 3) Update: After the m -th round selection, the users in the $\mu(m)$ cluster are informed to keep silent afterwards, i.e., setting $\mathcal{K}(m+1) = \mathcal{K}(m) \setminus \mu(m)$ and $m = m + 1$.
- 4) End control: If $m \leq \text{III}$, go to step 2; else, end.

After the selections, the indices of the selected users are collected in $J_D = \{j_{\mu(1)}^\dagger, j_{\mu(2)}^\dagger, j_{\mu(3)}^\dagger\}$. As shown in Fig. 3, the proposed RSS-based scheduling is able to generate the favorable patterns of characteristic directions, i.e., $\{\mathbf{r}_{j_k}\}_{k=1}^3$ are respectively aligned with distinct directions of $\{\mathbf{e}_m\}_{m=1}^{\text{III}}$. Then the channels as well as the SSA-resultant signal space are shaped under the guidance of RSS.

Next, the detailed implementations of the 2) and 3) steps of the proposed distributed CS are further elaborated. It is assumed that all the users are synchronized to a common clock, such as the Global Positioning System (GPS) signal, and a timer that lasts proportionally to $\phi_{j_k, m}$ is installed in S_{j_k} . More specifically, with the clock period T , the response time of the timer

of S_{j_k} , i.e., $\delta_{j_k,m}$, can be defined as $\delta_{j_k,m} = \frac{\phi_{j_k,m}}{90^\circ}T$. During the m -th round, R broadcasts a beacon signal with the index of the successful candidate of the $(m-1)$ -th round, i.e., $J_{\mu(m-1)}^\ddagger$, and $J_{\mu(0)}^\ddagger = \text{null}$. Upon receiving the beacon, each user first checks if $\mu(m-1)$ equals to its own cluster-index. If so, the user keeps silent for the rest of the scheduling period; if not, the user tries to compete during this round. The competing user S_{j_k} obtains the value of m from its own counter, and calculates $\delta_{j_k,m}$ to trigger the timer for the response to the beacon. The first time-out user is selected in each round.

Remark 1: The distributed CS enjoys very low implementation complexity without explicit feedback from the users. Although a relatively large number of candidates are necessary to achieve a distinct performance gain, the proposed scheme still enjoys a good performance-complexity tradeoff for the considered scenario. It is noted that the analysis of the number of candidates and the achievable performance gain is very challenging. The obstacle is the unknown statistical behaviour of the SSA-result signal space \mathbf{F} when user scheduling is considered [32]. It will be shown later that the system overhead is fixed for the proposed distributed CS, which is independent to the number of candidate users. In contrast, the complexity and CSI overheads of the centralized CS increase very fast as the number of users increases.

2) *RSS-based distributed GS:* Similar to the aforementioned CS, the proposed distributed GS relies on the angular-coordinate calculated by each user with RSS and local CSI. It is noted that the GS always needs a certain metric to evaluate the *group performance*, which requires the *centralized decision*. Still, the proposed scheme aims to *distribute the computations* to the users, so that the scheduling center R can be designed as simple as possible. In particular, the RSS-based distributed GS employs a progressive feedback protocol, which consists of two phases. In the first phase, $S_{j'_k}$ uses local CSI to check which direction of RSS is mostly aligned with its characteristic direction $\mathbf{r}_{j'_k}$, and feeds back the index of the most aligned RSS direction (using only two bits) to R as

$$m_{j'_k} = \arg \min_{m \in \{\text{I,II,III}\}} (\phi_{j'_k,m}). \quad (16)$$

Then R collects the indices of each group J' in a set $M_{J'} = \{m_{j'_1}, m_{j'_2}, m_{j'_3}\}$, and check if the elements in $M_{J'}$ have distinctive values. This checking serves as a coarse judgment on the orthogonality of the SSA-resultant signal space \mathbf{F} , and only when the elements in $M_{J'}$ are of distinctive values the related users continue to compete the channel. To offer some intuitions, Fig. 3 offers two user combinations, namely $\{S_{1_1}, S_{1_2}, S_{1_3}\}$ and $\{S_{2_1}, S_{2_2}, S_{2_3}\}$. The first combination can pass the coarse selection; but the second can not, since both \mathbf{r}_{2_1} and \mathbf{r}_{2_2} are more aligned with \mathbf{e}_1 . Let us collect the surviving groups in a set $\mathcal{J}'' \subseteq \mathcal{J}'$, in the second phase, R informs

each surviving user to feed back the individual scheduling metric, which is the smallest angle of its angular-coordinate within RSS, i.e.,

$$\phi_{j'_k, \min} = \min_{m \in \{I, II, III\}} (\phi_{j'_k, m}), j'_k \in J' \in \mathcal{J}''.$$
 (17)

Then R synthesizes $\{\phi_{j'_k, \min}\}_{k=1}^3$ to generate the GS scheduling metric $\phi_{sum}^{(J')} = \sum_{j'_k \in J'} \phi_{j'_k, \min}$ of one surviving group $J' \in \mathcal{J}''$, and the preferred user group is selected as

$$J'_D = \{j'_1, j'_2, j'_3\} = \arg \min_{J' \in \mathcal{J}''} (\phi_{sum}^{(J')}).$$
 (18)

Finally, it is noted that if no surviving users exist after the first phase, random selection can be used to pick one group out of \mathcal{J}' .

Remark 2: The progressive feedback is an opportunistic feedback scheme, which enables the distributed GS with low system overheads. Noting the symmetry of the channel's statistic properties, it is easy to check that the characteristic directions have equal chances to align with every direction in \mathbf{E} of RSS, then the *average surviving ratio* of a candidate group can be calculated as $3!/3^3 = 2/9$ after the first round of feedback on the aligned direction within RSS (16). Therefore, only 2/9 of the user groups need feed back the scheduling metrics (17) on average. In this sense, the proposed GS is suitable for the networks where the candidates are abundant and the low-complexity scheduling is demanded.

Remark 3: In fact, the proposed distributed CS/GS can only *shape* the SSA-result signal space \mathbf{F} , which is not a straightforward optimization towards the post-processing SNR. Since \mathbf{F} is coupled with the three-party channels within a user group, any further descriptions on \mathbf{F} may require the three-party CSI. To this end, it seems that shaping \mathbf{F} is perhaps the best thing one can do with local CSI and RSS. It is noted that the statistical behavior of \mathbf{F} is unknown with user scheduling in general [32], and also because of the reasons explained by Remark 4 below, we do not perform theoretical analysis on CS and GS with Min-UA transmission in this paper.

Remark 4: Similar to the distributed CS, the distributed GS with Min-UA transmission can only harvest partial MuD gain when the number of candidate groups is large; and the performance gap between the centralized and distributed scheduling schemes are distinct, which will be shown later in Section VI. These observations motivate us to look into the ER-UA case, where near-optimal distributed scheduling is possible as shown in the following sections.

D. RSS-based Distributed scheduling with Min-UA for $N > 1$

With a slight modification, the proposed distributed CS and GS with Min-UA can be extended to a more general system model, where each $2N$ -antenna user transmits $2N$ data streams via a $3N$ -antenna R, $N > 1$. Following the same idea in Subsection III-C, we choose the user group to shape \mathbf{F} with the help of RSS \mathbf{E} and local CSI. Specifically, the characteristic subspace instead of characteristic direction of user S_{j_k} is introduced as $\mathbf{R}_{j_k} \in \text{Null}(\mathbf{H}_{j_k})$, where $\mathbf{R}_{j_k} \in \mathbb{C}^{3N \times N}$ and $\mathbf{R}_{j_k}^H \mathbf{R}_{j_k} = \mathbf{I}_{N \times N}$. Furthermore, the chordal distance $d_c(\mathbf{A}, \mathbf{B})$ is used as an orthogonality measure of the two subspaces \mathbf{A} and \mathbf{B} , where $d_c(\mathbf{A}, \mathbf{B}) = \sqrt{N_T - \text{trace}(\mathbf{A}\mathbf{A}^H\mathbf{B}\mathbf{B}^H)}$ and $\mathbf{A}, \mathbf{B} \in \mathbb{C}^{N_R \times N_T}$ are generator matrices satisfying $\mathbf{A}^H\mathbf{A} = \mathbf{B}^H\mathbf{B} = \mathbf{I}_{N_T \times N_T}$ [36]. The larger value of $d_c(\mathbf{A}, \mathbf{B})$ represents the better orthogonality of \mathbf{A} and \mathbf{B} . For the procedure of distributed CS or GS with $N > 1$, the angular-coordinate of S_{j_k} is replaced by the chordal distance coordinate, i.e., $\phi_{j_k} = [\phi_{j_k, \text{I}}, \phi_{j_k, \text{II}}, \phi_{j_k, \text{III}}]$, where $\phi_{j_k, m} = d_c(\mathbf{R}_{j_k}, \mathbf{E}_m)$. Then, the distributed CS and GS can be carried out for $N > 1$ with the newly defined ϕ_{j_k} and the same procedures in the previous subsections.

Remark 5: It is worth pointing out that, in the scenario of $N > 1$, the performance improvement of the distributed CS with Min-UA transmission is not obvious as the number of candidate increases, especially for the distributed GS, which will be shown later in Section VI. In this scenario with high-dimensional signal space, it is very difficult to precisely characterize the orthogonality between subspaces or the intersection spaces with local CSI, which limits the performance of the proposed distributed scheduling schemes. Designing more effective low-complexity scheduling schemes for Min-UA transmission with $N > 1$ will be an interesting topic for future research.

IV. DISTRIBUTED SCHEDULING WITH ER-UA TRANSMISSION

In this section, the distributed user scheduling schemes are proposed for ER-UA transmission, where both relay and users are equally equipped with $N_T = N_R = 3N$ antennas. As compared with the Min-UA transmission, N extra antennas are added at the users, which offers enough dimensions to achieve an active signal alignment with predefined direction. Specifically, by venturing N extra antennas to each user, the application of RSS can be extended to guide both distributed beamforming and user scheduling. Moreover, it is interesting to note that, unlike the scheduling with Min-UA transmission, the distributed user scheduling schemes achieve

comparable performances as their centralized counterparts with ER-UA transmission. Again, the transmission scheme is first introduced before presenting the user scheduling schemes.

A. ER-UA MIMO-Y Transmission

Again, let us assume three users $\{S_1, S_2, S_3\}$ are randomly selected to exchange information. It is noted that the ER-UA MIMO-Y transmission relies on the RSS, which enables each user to design its transmit beamforming vectors with only local CSI and achieve SSA at the relay. Specifically, aiming at the pair-wise signal alignment in RSS Ω_R at R, the reference direction $\mathbf{e}_m^{[n]}$ is allocated to guide the pair-wise transmit beamforming of the n -th data stream at S_k and S_l , where $m = \pi(l, k)$ and $n \in [1, N]$. Note that the RSS-guided transmit beamforming vectors $\mathbf{v}_{l,k}^{[n]}$ and $\mathbf{v}_{k,l}^{[n]}$ can be solved separately with local CSI as

$$\mathbf{v}_{l,k}^{[n]} = \sqrt{P_T/2N} \langle \mathbf{H}_k^{-1} \mathbf{e}_m^{[n]} \rangle, \mathbf{v}_{k,l}^{[n]} = \sqrt{P_T/2N} \langle \mathbf{H}_l^{-1} \mathbf{e}_m^{[n]} \rangle, \quad (19)$$

and the power constraint is imposed as $\|\mathbf{v}_{l,k}^{[n]}\|^2 = \|\mathbf{v}_{k,l}^{[n]}\|^2 = P_T/2N$ per data stream. During the MAC phase, it is observed that SSA is achieved under the RSS, i.e., $\text{Span}(\mathbf{H}_k \mathbf{v}_{l,k}^{[n]}) = \text{Span}(\mathbf{H}_l \mathbf{v}_{k,l}^{[n]}) = \text{Span}(\mathbf{e}_m^{[n]})$, as shown in Fig. 4 with $N = 1$. the received signal at R (cf. (1)) is given by

$$\mathbf{y}_R = \sqrt{P_T/2N} \mathbf{E} \tilde{\mathbf{d}}_+ + \mathbf{n}_R, \quad (20)$$

where $\tilde{\mathbf{d}}_+ := [\tilde{\mathbf{d}}_{+,I}^T, \tilde{\mathbf{d}}_{+,II}^T, \tilde{\mathbf{d}}_{+,III}^T]^T \in \mathbb{C}^{3N \times 1}$ is the vector of the superimposed signals and $\mathbf{E} = [\mathbf{E}_I, \mathbf{E}_{II}, \mathbf{E}_{III}] \in \mathbb{C}^{N_R \times N_R}$ is the RSS as well as the equivalent MIMO channel seen by R. The m -th component of $\tilde{\mathbf{d}}_+$ is $\tilde{\mathbf{d}}_{+,m} = [\tilde{d}_{+,m}^{[1]}, \tilde{d}_{+,m}^{[2]}, \dots, \tilde{d}_{+,m}^{[N]}]^T \in \mathbb{C}^{N \times 1}$, where $\tilde{d}_{+,m}^{[n]} = \tilde{d}_{l,k}^{[n]} + \tilde{d}_{k,l}^{[n]}$, $\tilde{d}_{l,k}^{[n]} = \alpha_{m,k}^{[n]} d_{l,k}^{[n]}$, $m = \pi(l, k)$, and $\alpha_{m,k}^{[n]} = \|\mathbf{H}_k^{-1} \mathbf{e}_m^{[n]}\|^{-1}$ is the equivalent channel coefficient for $d_{l,k}^{[n]}$ in the MAC phase. Specifically, the equivalent channel gain (ECG) of $d_{l,k}^{[n]}$ is defined as $(\alpha_{m,k}^{[n]})^2 = \|\mathbf{H}_k^{-1} \mathbf{e}_m^{[n]}\|^{-2}$. Aiming at a simpler implementation, the fixed-gain AF relay is used here. The relay processing matrix is then simplified as $\tilde{\mathbf{W}} = \mathbf{I}_{N_R \times N_R}$. During the BC phase, the relay transmits $\mathbf{s}_R = G_R \mathbf{y}_R$ with the long-term power controlling coefficient

$$G_R = \sqrt{P_R/E \{ \|\mathbf{y}_R\|^2 \}} = \sqrt{2N P_R / (P_T \bar{\alpha}_{sum}^2 + 2N N_R \sigma_R^2)} = \sqrt{P_R/3 (P_T + N \sigma_R^2)}, \quad (21)$$

where $\bar{\alpha}_{sum}^2 = \sum_{k=1}^3 \sum_{l \in \mathcal{L}_k} \sum_{n=1}^N (\alpha_{\pi(l,k),k}^{[n]})^2 = 6N$, and $(\alpha_{m,k}^{[n]})^2 = E \left\{ \|\mathbf{H}_k^{-1} \mathbf{e}_m^{[n]}\|^{-2} \right\} = 1$ is the channel-averaged equivalent channel gain for $d_{l,k}^{[n]}$, which is calculated by employing the distribution of $(\alpha_{m,k}^{[n]})^2$ (see Lemma 4 in Appendix). Note that $(\alpha_{m,k}^{[n]})^2$ is only related to the long-term channel statistics and can be calculated, G_R is thus treated as a constant and

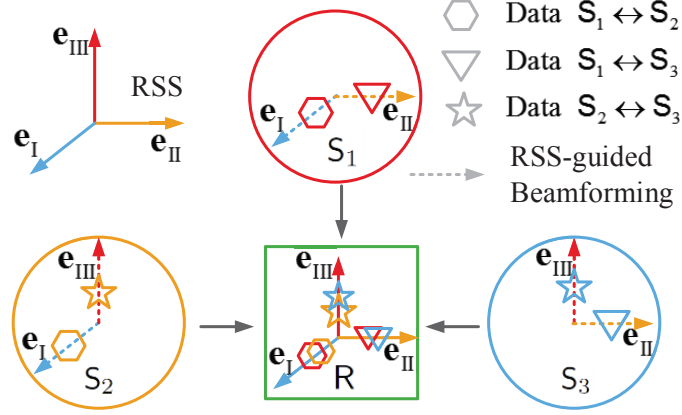


Fig. 4. Geometrical interpretation on the ER-UA transmission. After the RSS-guided beamforming, the signals are pair-wisely aligned with the basis of RSS at the relay during the MAC phase. The aligned directions are orthogonal, and the equivalent MIMO channel seen by the relay is well-conditioned.

assumed to be known by all the nodes in this network. Then the self-interference-free signal $\tilde{\mathbf{y}}_k = \mathbf{y}_k - G_R \mathbf{H}_k^H \mathbf{I} \mathbf{H}_k \mathbf{s}_k$ at S_k is expanded as

$$\tilde{\mathbf{y}}_k = \sqrt{P_T/2d} G_R \mathbf{H}_k^H \check{\mathbf{E}}_k \check{\mathbf{d}}_{+,k} + G_R \mathbf{H}_k^H \mathbf{n}_R + \mathbf{n}_k, \quad (22)$$

where $\check{\mathbf{E}}_k = [\mathbf{E}_{m_1} \mathbf{E}_{m_2} \mathbf{E}_{m'}] \in \mathbb{C}^{N_R \times N_R}$, and $\check{\mathbf{d}}_{+,k} = [\tilde{\mathbf{d}}_{k,l_1} \tilde{\mathbf{d}}_{k,l_2} \tilde{\mathbf{d}}_{+,m'}]^T \in \mathbb{C}^{N_T \times 1}$, $m_1 = \pi(l_1, k)$, $m_2 = \pi(l_2, k)$, $l_1, l_2 \in \mathcal{L}_k$ and $m' \in \{\text{I, II, III}\} \setminus \{m_1, m_2\}$. Based on (22), the receive beamforming $\mathbf{U}_k = G_R^{-1} [\mathbf{H}_k^{-1} \mathbf{E}_{m_1} \mathbf{H}_k^{-1} \mathbf{E}_{m_2}] \in \mathbb{C}^{N_T \times 2N}$ is used to obtain $\hat{\mathbf{y}}_k = \mathbf{U}_k^H \tilde{\mathbf{y}}_k$, and each desired signal stream within $\hat{\mathbf{y}}_k$ is given by

$$\hat{y}_{k,l}^{[n]} = \sqrt{P_T/2N} \alpha_{m,l}^{[n]} d_{k,l}^{[n]} + n_{k,l}^{[n]}, \quad l \in \mathcal{L}_k, n \in [1, N], \quad (23)$$

where $n_{k,l}^{[n]} = (\mathbf{e}_m^{[n]})^H \mathbf{n}_R + \frac{1}{G_R} (\mathbf{e}_m^{[n]})^H (\mathbf{H}_k^{-1})^H \mathbf{n}_k$ is the noise item. Then it is easy to extract the useful information from $\hat{y}_{k,l}^{[n]}$.

Remark 6: It is noted that the Min-UA transmission scheme requires *joint* transmit/receive beamforming design with the *three-party* CSI at users and relay, which involves high CSI overheads and relatively complicated signal processing. In contrast to Min-UA, ER-UA transmission employs extra user antennas to enable the simple RSS-based *distributed* transmit/receive beamforming design with *local* CSI. Therefore, the system overhead for CSI exchanging is significantly reduced. Another advantage of ER-UA transmission is that it enables the near-optimal and low-complexity RSS-based distributed user scheduling, which will be shown in the next subsection.

B. Problem Formulation and Centralized Scheduling

Similar to Section III-B⁸, the user index set $J = \{j_1, j_2, j_3\}$ is re-introduced and the relevant overall outage probability is defined as $P_{out}^{(J)}(\rho_{th}) = \Pr\left(\rho_{min}^{(J)} \leq \rho_{th}\right)$ and the overall post-processing SNR is defined as $\rho_{min}^{(J)} = \min_{k \in [1,3], l \in \mathcal{L}_k, n \in [1,d]} \left(\rho_{j_k, j_l}^{[n]}\right)$, where $\rho_{j_k, j_l}^{[n]}$ is the end-to-end post-processing SNR of the n -th data stream within the link $S_{j_l} \rightarrow R \rightarrow S_{j_k}$, $l \in \mathcal{L}_k$. From (23), $\rho_{j_k, j_l}^{[n]} = \mathbb{E} \left\{ \left(\sqrt{P_T/2N} \alpha_{m,l}^{[n]} d_{k,l}^{[n]} \right)^2 \right\} / \mathbb{E} \left\{ \left(n_{k,l}^{[n]} \right)^2 \right\}$ is calculated as

$$\rho_{j_k, j_l}^{[n]} = \frac{1}{2N} \times \frac{\rho_{j_k, j_l, 2}^{[n]} \rho_{j_k, j_l, 1}^{[n]}}{\rho_{j_k, j_l, 2}^{[n]} + 3(\text{SNR}_T + N)}, \quad (24)$$

where $\rho_{j_k, j_l, 1}^{[n]} = \text{SNR}_T \left(\alpha_{m, j_l}^{[n]} \right)^2$ and $\rho_{j_k, j_l, 2}^{[n]} = \text{SNR}_R \left(\alpha_{m, j_k}^{[n]} \right)^2$ are treated as the equivalent SNRs of the first hop and second hop. After introducing necessary notations, the centralized CS and GS are first considered as benchmarks, which are respectively given by

$$J_C = \{j_1^*, j_2^*, j_3^*\} = \arg \max_{J \in \mathcal{J}} \left(\rho_{min}^{(J)} \right), \quad (25)$$

and

$$J'_C = \{j'_1, j'_2, j'_3\} = \arg \max_{J' \in \mathcal{J}'} \left(\rho_{min}^{(J')} \right). \quad (26)$$

Again, it is noted that the CSI overheads and the computational complexities involved in the centralized CS and GS are high. To this end, a simplified scheduling is required.

C. RSS-based Distributed User Scheduling with ER-UA

In this subsection, RSS-based distributed CS and GS are proposed with ER-UA transmission. It is noted that, employing the RSS-based beamforming the MIMO channel can be decoupled and the SSA-resultant signal space is same as the RSS \mathbf{E} . Moreover, the end-to-end link SNR of one data stream in (24) is an increasing function of the two equivalent channel gains (ECGs) defined in Section IV-A, $\left(\alpha_{m, j_l}^{[n]} \right)^2$ and $\left(\alpha_{m, j_k}^{[n]} \right)^2$, where each ECG is only determined by the local CSI \mathbf{H}_{j_k} (\mathbf{H}_{j_l}) and RSS. Based on this observation, we propose disturbed user scheduling to maximize the ECG as well as the end-to-end SNR. Intuitively, the considered distributed scheduling exploits the symmetry of the reciprocal bi-directional channel. An example is give by Fig. 5, where the first-hop of $S_k \xrightarrow{1st} R \xrightarrow{2nd} S_l$ is optimized for the k -th cluster, the second-hop of $S_l \xrightarrow{1st} R \xrightarrow{2nd} S_k$ is analogously optimized for the l -th cluster. Therefore, efficient distributed implementations of CS and GS are possible with ER-UA and RSS, which are detailed in the following subsections.

⁸We may reuse some of the notations appeared in the previous sections to convey similar concepts, if not causing confusion.

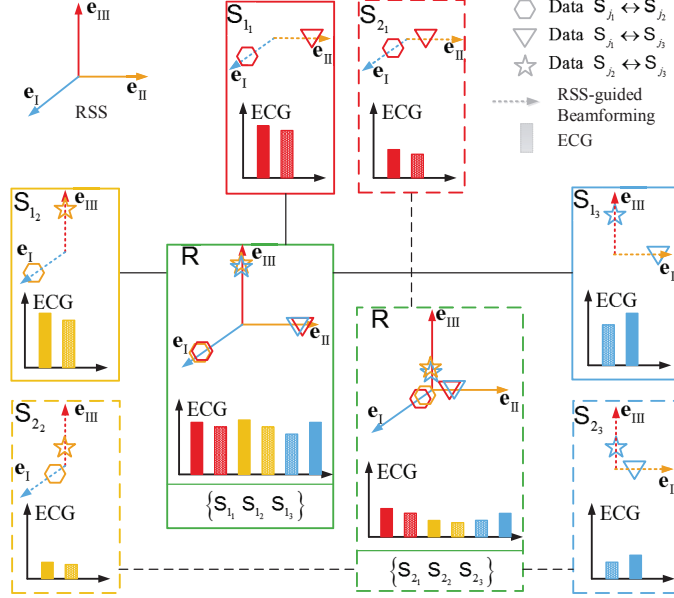


Fig. 5. The geometrical interpretations on the RSS-based distributed user scheduling with ER-UA transmission. In this example, we consider the cluster-wise scheduling and assume that there are two users $\{S_{1k}, S_{2k}\}$ in the k -th cluster, $k \in [1, 3]$. Due to the RSS-guided transmit beamforming design, each user can predict the ECG of its own signals before their arrival at the relay. Employing the proposed distributed user scheduling, the minimum ECG at the relay can be directly improved.

1) *RSS-based Distributed CS*: Employing RSS, each user can not only design its transmit beamforming as (19) to ensure SSA at the relay, but also calculate the scheduling metric, i.e., the minimum-ECG, to enable distributed CS. In particular, the minimum-ECG of S_{j_k} is defined as $\alpha_{j_k}^2 = \min_{n \in [1, N]} \left(\min \left(\left(\alpha_{m_1, j_k}^{[n]} \right)^2, \left(\alpha_{m_2, j_k}^{[n]} \right)^2 \right) \right)$, $m_1 = \pi(l_1, k)$, $m_2 = \pi(l_2, k)$, and $\left(\alpha_{m_1, j_k}^{[n]} \right)^2$ and $\left(\alpha_{m_2, j_k}^{[n]} \right)^2$ are the ECGs, which are defined in Section IV A, for $d_{l_1, k}^{[n]}$ and $d_{l_2, k}^{[n]}$ separately. $\alpha_{j_k}^2$ can be calculated with the local CSI \mathbf{H}_{j_k} and RSS. It is noted the RSS-based distributed CS is independently conducted in each cluster, which aims to find the user with the maximal minimum-ECG from each cluster, as shown in Fig. 5. Then, the efficient distributed scheduling is given by $J_D = \{j_1^\ddagger, j_2^\ddagger, j_3^\ddagger\}$, where the preferable user of the k -th cluster is selected according to the following criterion

$$j_k^\ddagger = \arg \max_{j_k \in [1, M_k]} (\alpha_{j_k}^2). \quad (27)$$

The distributed implementation of the proposed scheme is simple. Similar to distributed CS with Min-UA transmission, we assume all users are synchronized to a common clock. To start the scheduling, R broadcasts a beacon and S_{j_k} calculates $\alpha_{j_k}^2$ with local CSI \mathbf{H}_{j_k} ; then a timer

that lasts inverse-proportionally to $\alpha_{j_k}^2$ is used by S_{j_k} . Specifically, with the clock period T , the response time of the timer of S_{j_k} , i.e., δ'_{j_k} can be defined as $\delta'_{j_k} = \frac{1}{\alpha_{j_k}^2}T$. Then, the competing user S_{j_k} calculates δ_{j_k} to trigger the timer for the response to the beacon. The first time-out user must be $S_{j_k^\ddagger}$.

2) *RSS-based Distributed GS*: Similar to the Min-UA scenario, for the distributed GS with ER-UA transmission, each user exploits local CSI to calculate the individual scheduling metric and feeds it back to R for final decision. The distributed GS is first given by

$$J'_D = \{j_1^{\ddagger}, j_2^{\ddagger}, j_3^{\ddagger}\} = \arg \max_{J' \in \mathcal{J}'} \left(\gamma_{min}^{(J')} \right), \quad (28)$$

where $\gamma_{min}^{(J')} = \frac{1}{2N} \frac{\text{SNR}_T \left(\alpha_{[3]}^{(J')} \right)^2 \text{SNR}_R \left(\alpha_{[2]}^{(J')} \right)^2}{\text{SNR}_R \left(\alpha_{[2]}^{(J')} \right)^2 + 3(\text{SNR}_T + N)}$ is the GS metric synthesized by R and is defined as the equivalent SNR of the user group J' , and $\alpha_{[n]}^{(J')}$ is the n -th largest element of $\{\alpha_{j_1}, \alpha_{j_2}, \alpha_{j_3}\}$. It is noted that user S_{j_k} can calculate $\alpha_{j_k}^2$ with local CSI, and the value is fed back to the relay R. With a total of $3M$ feedback of individual metrics, R forms the set $\left\{ \gamma_{min}^{(J'_p)} \right\}_{p=1}^M$ and makes a centralized decision to choose the preferred user group.

Remark 7: The individual scheduling metric and the synthesized GS metric are critical. In the proposed distributed GS, $\alpha_{j_k}^2$ characterizes the quality of the weaker link between S_k and R, and $\gamma_{min}^{(J')}$ is actually constructed as a lower bound of $\rho_{min}^{(J')}$ to be shown later. Therefore, the distributed GS aims to improve the lower bound of the overall system performance.

Remark 8: Unlike the scheduling schemes with the Min-UA transmission, the proposed distributed CS and GS achieve comparable performances as their centralized counterparts with the ER-UA; therefore, the proposed distributed scheduling schemes enjoy very good performance-complexity tradeoffs with the ER-UA. In the next section, these observations are theoretically analyzed.

Remark 9: For Min-UA transmission, the scheduling metrics of the distributed CS and GS are determined by the angular-coordinate ϕ_{j_k} . Due to the symmetrical random property of the considered wireless channel, the distribution of ϕ_{j_k} is identical for different j_k ; therefore, each user or user group have the same opportunity to be selected on the long-term. For ER-UA transmission, the scheduling metrics of the distributed CS and GS are determined by the minimum-ECG α_{j_k} . It is easy to check that for the considered scenarios, the distribution of α_{j_k} is identical for different j_k ; therefore, the the long-term fairness can also be guaranteed.

V. PERFORMANCE ANALYSIS WITH ER-UA TRANSMISSION

In this section, outage performances of the proposed distributed CS, GS and their centralized counterparts are quantified with ER-UA transmission. Since we are mainly interested in the MuD orders, we assume $N = 1$, $\text{SNR}_R = \text{SNR}_T = \text{SNR}$ and $M_1 \leq M_2 \leq M_3$ to ease the derivations. Note that $N = 1$, the RSS and the ECG is simplified as $\mathbf{E} = [\mathbf{e}_I \mathbf{e}_{II} \mathbf{e}_{III}] \in \mathbb{C}^{3 \times 3}$ and $\alpha_{m,j_k}^2 = \|\mathbf{H}_{j_k}^{-1} \mathbf{e}_m\|^{-2}$, respectively. In order to facilitate the analysis, let us denote the min-SNRs (cf. (10)) of centralized CS (25) and GS (26) as $\rho_{min,CS}^{(J_C)}$ and $\rho_{min,GS}^{(J'_C)}$; similarly, we denote the min-SNRs of distributed CS (27) and GS (28) as $\rho_{min,CS}^{(J_D)}$ and $\rho_{min,GS}^{(J'_D)}$. It is noted that the analysis of the distributed scheduling schemes is difficult, because the optimization objectives of these schemes are not exactly the min-SNRs of the network. To this end, tractable lower bounds (LB) and upper bounds (UB) are first established for 1) $\rho_{min,CS}^{(J_C)}$ and $\rho_{min,CS}^{(J_D)}$ with CS, then for 2) $\rho_{min,GS}^{(J'_C)}$ and $\rho_{min,GS}^{(J'_D)}$ with GS, respectively. Next, the bounds of outage probabilities are developed with tractable theoretical results, and their high SNR approximations are analyzed to extract the DMT and MuD orders.

A. Bounding the outage probabilities

To begin with, the following proposition is introduced to bound the min-SNRs with CS.

Proposition 1. Using ER-UA transmission, the min-SNRs of centralized and distributed CS are bounded as

$$\rho_{min,CS}^{LB} \stackrel{(a1)}{\leq} \rho_{min,CS}^{(J_D)} \stackrel{(a2)}{\leq} \rho_{min,CS}^{(J_C)} \stackrel{(a3)}{\leq} \rho_{min,CS}^{UB}, \quad (29)$$

where the LB and UB are $\rho_{min,CS}^{LB} = g\left(\tilde{\lambda}_{[3]}^{(J_\lambda)}, \tilde{\lambda}_{[2]}^{(J_\lambda)}\right)$ and $\rho_{min,CS}^{UB} = g\left(\alpha_{1,j_1^\dagger}^2, \alpha_{1,j_2^\dagger}^2\right)$, respectively, and $g(x, y) := \frac{xy\text{SNR}}{2y+6(1+\text{SNR}^{-1})}$, $x, y > 0$. For $\rho_{min,CS}^{LB}$, $\tilde{\lambda}_{[n]}^{(J_\lambda)}$ is the n -th largest element of $\left\{\tilde{\lambda}_{j_1^\dagger}, \tilde{\lambda}_{j_2^\dagger}, \tilde{\lambda}_{j_3^\dagger}\right\}$, where $J_\lambda = \{j_1^\dagger, j_2^\dagger, j_3^\dagger\}$, $j_k^\dagger = \arg \max_{j_k \in [1, M_k]} \left(\tilde{\lambda}_{j_k}\right)$ and $\tilde{\lambda}_{j_k} = \lambda_{min}\left(\mathbf{H}_{j_k} \mathbf{H}_{j_k}^H\right)$, $j_k \in [1, M_k]$. For $\rho_{min,CS}^{UB}$, $j_k^\dagger = \arg \max_{j_k \in [1, M_k]} \left(\alpha_{1,j_k}^2\right)$, $k = 1, 2$.

Proof: See Appendix I. ■

Similarly, the following proposition is used to bound the min-SNRs with GS.

Proposition 2. Using ER-UA transmission, the min-SNRs of centralized GS and distributed GS are bounded as

$$\rho_{min,GS}^{LB} \stackrel{(b1)}{\leq} \rho_{min,GS}^{(J'_D)} \stackrel{(b2)}{\leq} \rho_{min,GS}^{(J'_C)} \stackrel{(b3)}{\leq} \rho_{min,GS}^{UB}, \quad (30)$$

where the LB and UB are $\rho_{min,GS}^{LB} = \max_{J' \in \mathcal{J}'} \left\{ g \left(\tilde{\lambda}_{[3]}^{(J')}, \tilde{\lambda}_{[2]}^{(J')} \right) \right\}$ and $\rho_{min,GS}^{UB} = g \left(\alpha_{1,j_1^\dagger}^2, \alpha_{1,j_2^\dagger}^2 \right)$, respectively. For $\rho_{min,GS}^{LB}$, $\tilde{\lambda}_{[n]}^{(J')}$ is the n -th largest element of $\left\{ \tilde{\lambda}_{j_1'}, \tilde{\lambda}_{j_2'}, \tilde{\lambda}_{j_3'} \right\}$, where $J' = \{j_1', j_2', j_3'\} \in \mathcal{J}'$, $\tilde{\lambda}_{j_k'} = \lambda_{min} \left(\mathbf{H}_{j_k'} \mathbf{H}_{j_k'}^H \right)$. For $\rho_{min,GS}^{UB}$, $j_k^\dagger = \arg \max_{j_k \in [1, M]} \left(\alpha_{1,j_k}^2 \right)$, $k = 1, 2$.

Proof: See Appendix II. ■

From Proposition 1 and Proposition 2, the *common* LB and UB for $P_{out,CS}^{(J_C)}$ and $P_{out,CS}^{(J_D)}$ with CS are defined as

$$P_{out,CS}^{LB} \leq P_{out,CS}^{(J_C)} \leq P_{out,CS}^{(J_D)} \leq P_{out,CS}^{UB}, \quad (31)$$

where $P_{out,CS}^{LB}(\rho_{th}) = \Pr \left(\rho_{min,CS}^{UB} \leq \rho_{th} \right)$, $P_{out,CS}^{UB}(\rho_{th}) = \Pr \left(\rho_{min,CS}^{LB} \leq \rho_{th} \right)$. And similarly, the common LB and UB for $P_{out,GS}^{(J_C)}$ and $P_{out,GS}^{(J_D)}$ with GS are given by

$$P_{out,GS}^{LB} \leq P_{out,GS}^{(J_C)} \leq P_{out,GS}^{(J_D)} \leq P_{out,GS}^{UB}, \quad (32)$$

where $P_{out,GS}^{LB}(\rho_{th}) = \Pr \left(\rho_{min,GS}^{UB} \leq \rho_{th} \right)$, $P_{out,GS}^{UB}(\rho_{th}) = \Pr \left(\rho_{min,GS}^{LB} \leq \rho_{th} \right)$. Then, these bounds are further quantified. Particularly, an ordered set $\mathcal{M}_\pi = \{\mathcal{M}_i\}_{i=1}^6$ is introduced to collect all the permutations of the three elements in $\mathcal{M}_i = \{M_1, M_2, M_3\}$, where \mathcal{M}_i is also an ordered set and the n -th element of \mathcal{M}_i is denoted as $M_{i,n}$, $n \in [1, 3]$. The detailed derivations are collected in Appendix III and the key results of $P_{out,CS}^{LB}(\rho_{th})$, $P_{out,CS}^{UB}(\rho_{th})$ and $P_{out,GS}^{UB}(\rho_{th})$ are given by

$$P_{out,CS(GS)}^{LB}(\rho_{th}) = 2M_2 \sum_{q=0}^{M_2-1} \left[\frac{(-1)^q \binom{M_2-1}{q}}{2(q+1)} + \sum_{p=1}^{M_1} \binom{M_2-1}{q} \binom{M_1}{p} (-1)^{q+p} e^{-pa} \sqrt{\frac{pb}{(q+1)}} K_1 \left(2\sqrt{p(q+1)b} \right) \right], \quad (33)$$

$$P_{out,CS}^{UB}(\rho_{th}) \approx \sum_{i=1}^6 \left(\frac{M_{i,2} M_{i,3} (1 - e^{-3\mu})^{M_\Sigma} + M_{i,2} M_\Sigma (1 - e^{-3\mu})^{M_{i,1} + M_{i,2}} \left[1 - (1 - e^{-3\mu})^{M_{i,3}} \right]}{(M_{i,1} + M_{i,2}) M_\Sigma} \right. \\ \left. + \left[3M_{i,2} \sum_{p=0}^{M_{i,2}-1} \sum_{q=0}^{M_{i,1}} (-1)^q \binom{M_{i,2}-1}{p} \binom{M_{i,1}}{q} e^{-3qa} \int_\mu^\infty e^{-3((p+1)y - qb\frac{1}{y})} dy \right] \left[1 - (1 - e^{-3\mu})^{M_{i,3}} \right] \right), \quad (34)$$

and

$$P_{out,GS}^{UB}(\rho_{th}) \approx \left[3(1 - e^{-3\mu})^2 - 2(1 - e^{-3\mu})^3 + 6 \left(e^{-6\mu} - 3e^{-3(\mu+a)} \int_\mu^\infty e^{-3[y - b\frac{1}{y}]} dy \right) \right]^M, \quad (35)$$

respectively, where $K_1(x)$ is the modified Bessel function of the second kind [37], $a(\rho_{th}) = \frac{2\rho_{th}}{\text{SNR}}$, $b(\rho_{th}) = \frac{6\rho_{th}(\text{SNR}+1)}{\text{SNR}^2}$ and $\mu = \frac{1}{2} \left(a + \sqrt{a^2 + 4b} \right)$ is the positive root of the quadratic equation $y^2 = ay + b$, $M_\Sigma = M_1 + M_2 + M_3$. It is noted that the integral $\int_\mu^\infty e^{-3[(p+1)y - qb\frac{1}{y}]} dy$ in (34) can be efficiently evaluated with software like MATLAB or Mathematica. Finally, it is noted that $P_{out,GS}^{LB}(\rho_{th})$ can be obtained from (33) by setting $M_1 = M_2 = M$, therefore, the equation of (33) is reused for conciseness.

B. High SNR Analysis

In this subsection, the high SNR analysis on the bounds of outage probabilities are given, including the asymptotic approximations and the DMT. Only the key results are provided here while all the derivations and proofs are collected in Appendix IV and Appendix V.

1) High SNR Approximations of $P_{out,CS}^{LB}$ and $P_{out,CS}^{UB}$:

a) $P_{out,CS}^{LB}$: high SNR approximation of $P_{out,CS}^{LB}(\rho_{th})$ is given as follows

$$\begin{cases} G_{CS,1}^{LB} \left(\frac{2\rho_{th}}{\text{SNR}} \right)^{d_{CS}^{UB}} \ln \left(\frac{\text{SNR}}{2\rho_{th}} \right), & M_{[2]} = M_{[3]}, \\ G_{CS,2}^{LB} \left(\frac{2\rho_{th}}{\text{SNR}} \right)^{d_{CS}^{UB}}, & M_{[2]} \neq M_{[3]}, \end{cases} \quad (36)$$

where the diversity UB is $d_{CS}^{UB} = M_{[3]}$, and the power gains are $G_{CS,1}^{LB} = M_{[3]}3^{M_{[3]}}$, $G_{CS,2}^{LB} = \varphi(M_{[3]}, M_{[2]}, 1)$. Here $M_{[n]}$ is the n -th largest element of $\{M_1, M_2, M_3\}$, and $\varphi(N_1, N_2, \tau)$ is given by

$$\varphi(N_1, N_2, \tau) = N_2 \sum_{q=0}^{N_2-1} \sum_{p=1}^{N_1} \frac{(-1)^{q+p} C_q^{N_2-1} C_p^{N_1} (\mathbf{c}_p^T(\tau) \mathbf{e}_{p,q}(\tau))}{(q+1)},$$

where $\mathbf{c}_p(\tau) = [c_{p,d'}(\tau), c_{p,d'-1}(\tau), \dots, 1]^T \in \mathbb{C}^{(d'+1) \times 1}$ with element $c_{p,n}(\tau) = \frac{(-\tau p)^n}{n!}$, $n \in [0, d']$, $d' = \min(N_1, N_2)$, and $\mathbf{e}_{p,q}(\tau) = [0, e_{p,q,1}(\tau), \dots, e_{p,q,d'}(\tau)]^T \in \mathbb{C}^{(d'+1) \times 1}$ with element

$$\begin{aligned} e_{p,q,n}(\tau) &= \left(b_{1,n-1} \ln \left(2\tau \sqrt{3p(q+1)} \right) + b_{2,n-1} \right) \\ &\quad \times (12\tau^2 p(q+1))^n, \quad n \in [1, d'], \end{aligned}$$

where the coefficients in $e_{p,q,n}(\tau)$ are $b_{1,t} = \frac{2^{-2t-1}}{t!(t+1)!}$, $b_{2,t} = b_{1,t} \left[-\ln(2) - \frac{1}{2}(\psi(t+1) + \psi(t+2)) \right]$, $t = n-1$, and $\psi(x)$ is the digamma function [37].

b) $P_{out,CS}^{UB}$: Then the high SNR approximation for $P_{out,CS}^{UB}(\rho_{th})$ is given as

$$\begin{cases} G_{CS,1}^{UB} \left(\frac{2\rho_{th}}{\text{SNR}} \right)^{d_{CS}^{LB}} \ln \left(\frac{\text{SNR}}{2\rho_{th}} \right), & M_{[1]} = M_{[2]} = M_{[3]}, \\ G_{CS,2}^{UB} \left(\frac{2\rho_{th}}{\text{SNR}} \right)^{d_{CS}^{LB}} \ln \left(\frac{\text{SNR}}{2\rho_{th}} \right), & M_{[1]} \geq M_{[2]} = M_{[3]}, \\ G_{CS,3}^{UB} \left(\frac{2\rho_{th}}{\text{SNR}} \right)^{d_{CS}^{LB}}, & M_{[1]} = M_{[2]} \geq M_{[3]}, \\ G_{CS,4}^{UB} \left(\frac{2\rho_{th}}{\text{SNR}} \right)^{d_{CS}^{LB}}, & M_{[1]} \neq M_{[2]} \neq M_{[3]}, \end{cases} \quad (37)$$

where the diversity LB is $d_{CS}^{LB} = M_{[3]}$, and the power gains are $G_{CS,1}^{UB} = 6M_{[3]}3^{3M_{[3]}}$, $G_{CS,2}^{UB} = 2M_{[3]}3^{3M_{[3]}}$, $G_{CS,3}^{UB} = \varphi(M_{[2]}, M_{[3]}, 3) + \varphi(M_{[3]}, M_{[2]}, 3)$, and $G_{CS,4}^{UB} = \sum_{l=1}^2 \varphi(M_{[l]}, M_{[3]}, 3) + \varphi(M_{[3]}, M_{[l]}, 3)$.

2) High SNR Approximations of $P_{out,GS}^{LB}$ and $P_{out,GS}^{UB}$:

a) $P_{out,GS}^{LB}$: As shown in (33), $P_{out,GS}^{LB}(\rho_{th}) = P_{out,CS}^{LB}(\rho_{th})$, when $M_{i \in [1,3]} = M$, then the high SNR approximation regarding $P_{out,CS}^{LB}(\rho_{th})$ in (36) can be modified to obtain

$$P_{out,GS}^{LB}(\rho_{th}) \approx G_{GS}^{LB} \left(\frac{2\rho_{th}}{\text{SNR}} \right)^{d_{GS}^{UB}} \ln \left(\frac{\text{SNR}}{2\rho_{th}} \right), \quad (38)$$

where $d_{GS}^{UB} = M$ and $G_{GS}^{LB} = M3^M$.

b) $P_{out,GS}^{LB}$: The derivations of $P_{out,GS}^{UB}(\rho_{th})$ are given in Appendix IV, and the result is given by

$$P_{out,GS}^{UB}(\rho_{th}) \approx G_{GS}^{UB} \left(\frac{2\rho_{th}}{\text{SNR}} \ln \left(\frac{\text{SNR}}{2\rho_{th}} \right) \right)^{d_{GS}^{LB}}, \quad (39)$$

where $d_{GS}^{UB} = M$ and $G_{GS}^{UB} = (6 \times 3^3)^M$.

3) *DMT Analysis*: In this subsection, the results of high SNR approximations are further generalized and unified within the DMT framework [34]. The DMT analysis gives a comprehensive description of the tradeoff between transmission reliability and spectral efficiency with adaptive data-rate. For the whole system with adaptive data-rate, a target sum-rate is defined as $R_{th}(\text{SNR}) = r \log_2(1 + \text{SNR})$ and r is the multiplexing gain. Then, the outage probability of the system is redefined with R_{th} as

$$P_{out}(\text{SNR}) = \Pr(R(\text{SNR}) \leq R_{th}(\text{SNR})), \quad (40)$$

where $R(\text{SNR}) = \frac{1}{2} \sum_{k \in [1,3]} \sum_{l \in \mathcal{L}_k} \log_2(1 + \rho_{k,l}(\text{SNR}))$ is the instantaneous sum-rate of the system, and $\rho_{k,l}$ is the end-to-end post-processing SNR of link $S_l \rightarrow R \rightarrow S_k$. Finally, the DMT is defined as

$$d(r) = - \lim_{\text{SNR} \rightarrow \infty} \frac{\log(P_{out}(\text{SNR}))}{\log(\text{SNR})}. \quad (41)$$

After these definitions, a proposition is given to summarize the DMT results.

Proposition 3. Using ER-UA transmission, both centralized CS and distributed CS achieve the same DMT as

$$d_{CS}(r) = \min(M_1, M_2, M_3)(1 - r/3)^+, \quad (42)$$

and both centralized GS and distributed GS achieve the same DMT as

$$d_{GS}(r) = M(1 - r/3)^+. \quad (43)$$

Proof: See Appendix V. ■

Remark 10: The maximum MuD orders are obtained as $d_{CS}^* = \min(M_1, M_2, M_3)$ for both distributed and centralized CS, and $d_{GS}^* = M$ for both distributed and centralized GS. If the random scheduling is employed, the maximum MuD order would be just 1. Therefore, the proposed schemes obtain scalable MuD orders. Moreover, by showing that both the outage-optimal centralized scheduling and the proposed distributed scheduling achieve the same DMT, the optimality of the proposed distributed scheduling schemes are established with ER-UA transmission. Finally, given a total number of candidates, it is shown that the symmetric user configuration is most efficient from the DMT's perspective, which equally distributes the candidates in three clusters.

VI. NUMERICAL RESULTS

In this section, numerical results are presented to show the effectiveness of the proposed schemes and validate the theoretical derivations. The i.i.d. Rayleigh fading channels are assumed. The overall outage probability is used as an effective metric to evaluate the transmission reliability of the network. Specifically, the SNR threshold is set as $\rho_{th} = 1$ for each unicast stream, which corresponds to a target rate of $0.5 \times 6N \times \log_2(1 + \rho_{th}) = 3N$ bit per channel use of the MIMO-Y channel. The symmetric SNR is assumed for the relay system as $P_T/\sigma_R^2 = P_R/\sigma_S^2 = \text{SNR}$. The triplet (M_1, M_2, M_3) is used to represent the number of users in all the three clusters, and it is simplified as (M) for the GS.

A. Performance and Complexity Comparisons

In this test case, we first compare both the distributed and the centralized scheduling schemes for the Min-UA and the ER-UA MIMO-Y transmissions with $N = 1$. Then we present the performance of distributed scheduling schemes for both transmissions with $N = 2$ to demonstrate the effectiveness of the proposed schemes in more general MIMO Y channels. The symmetric user configuration, i.e., (M, M, M) , is assumed. The random selection is used as a reference, which achieves a MuD order of 1 regardless the user configuration. Therefore, the random selection is also indicated by user configuration (1,1,1) for CS or simplified as (1) for GS.

1) *Min-UA Transmission for $N = 1$* : Focusing on the Min-UA transmission, Fig. 6 and Fig. 7 present the overall outage performances of the CS and the GS, respectively. It is observed that the proposed distributed scheduling schemes are inferior to the centralized schemes. Only when M is relatively large, the distributed scheduling shows distinctive performance improvement as compared to the random selection.

2) *ER-UA Transmission for $N = 1$* : Fig. 8 and Fig. 9 present the overall outage performances of CS and GS with ER-UA transmission. As shown in these figures, the proposed distributed user scheduling schemes and their centralized counterparts achieve comparable performances. Moreover, a scalable MuD order is observed for both the centralized scheduling and the proposed distributed scheduling. These observations prove the optimality of the distributed scheduling in terms of MuD order.

3) *Min-UA and ER-UA Transmissions for $N = 2$* : In order to validate the effectiveness of the proposed distributed scheduling schemes in more general MIMO Y channels, Fig. 10 presents

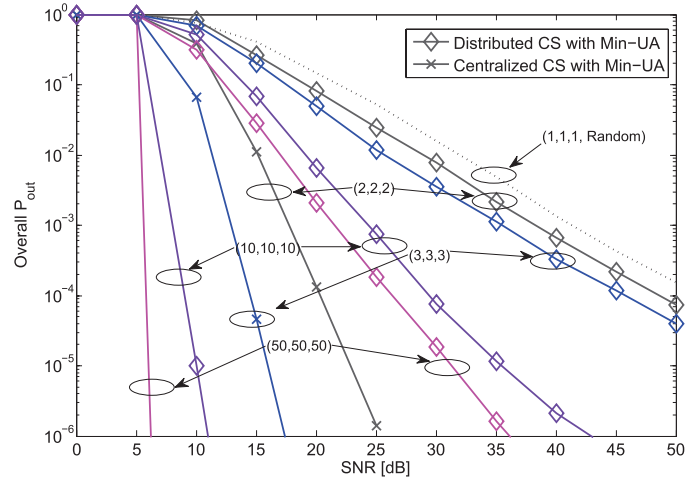


Fig. 6. Overall outage probability of the centralized and distributed CS with Min-UA transmission, where $N_R = 3$, $N_T = 2$ and $\rho_{th} = 1$.

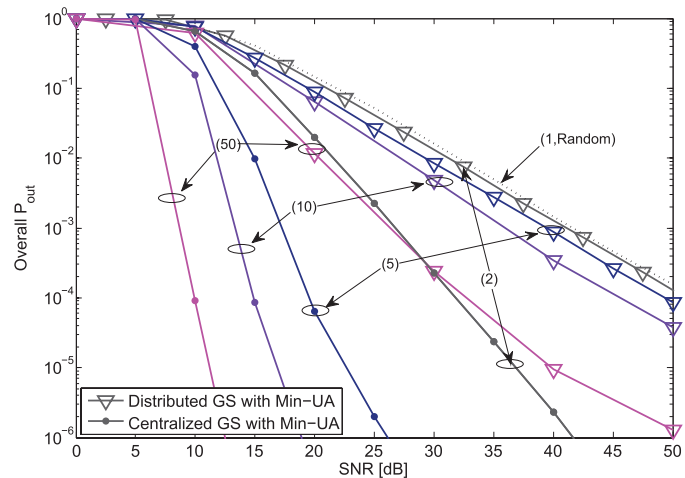


Fig. 7. Overall outage probability of the centralized and distributed GS with Min-UA transmission, where $N_R = 3$, $N_T = 2$ and $\rho_{th} = 1$.

the overall outage performances of the distributed scheduling schemes for Min-UA and ER-UA MIMO-Y transmissions with $N = 2$. For the Min-UA transmission, it is shown that the performance gains of CS and GS are not so evident. Especially in the GS case, the performance improvement is somewhat trivial. On the contrary, significant performance gain is achieved in CS and GS with ER-UA transmission, where a scalable MuD order is observed.

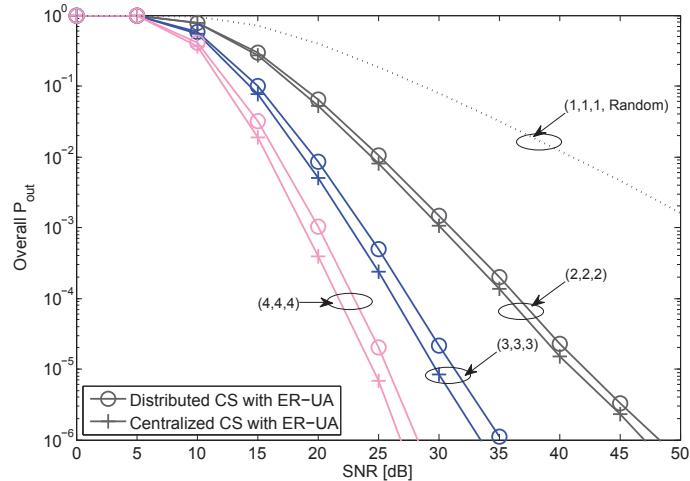


Fig. 8. Overall outage probability of the centralized and distributed CS with ER-UA transmission, where $N_R = N_T = 3$ and $\rho_{th} = 1$.

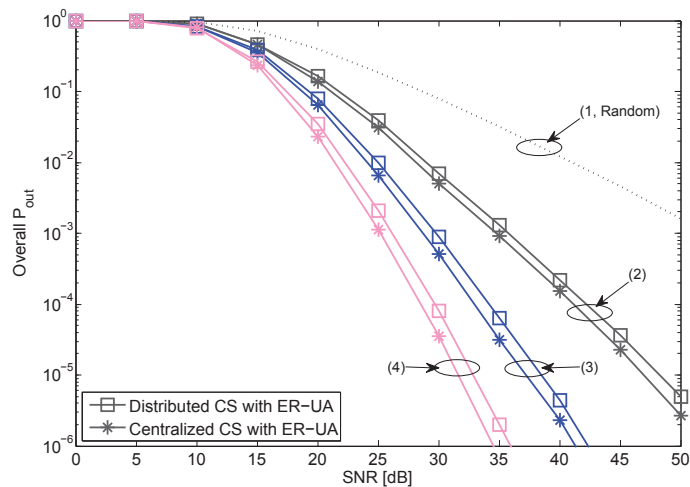


Fig. 9. Overall outage probability of the centralized and distributed GS with ER-UA transmission, where $N_R = N_T = 3$ and $\rho_{th} = 1$.

4) *Complexity and CSI Overhead*: To further appreciate the proposed distributed scheduling, the computational complexities and the CSI overheads of all the considered scheduling schemes are briefly analyzed and compared. The complexity is measured in terms of the number of floating point operations (flops) [36]. In particular, the complexity is presented in a manner

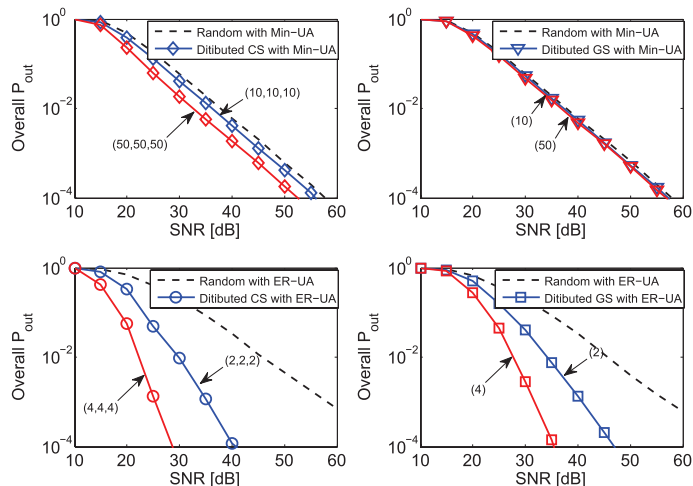


Fig. 10. Overall outage probability of the distributed scheduling schemes for the Min-UA and the ER-UA transmissions, where $N = 2$ and $\rho_{th} = 1$. Note that we set $N_R = 3N = 6$, $N_T = 2N = 4$ for Min-UA and $N_R = N_T = 3N = 6$ for ER-UA.

such that the distributed nature our proposed scheme can be highlighted⁹. As shown in Table I, the centralized scheduling schemes require global CSI of all the candidates, which involves high CSI feedback overheads. The computational complexity at the scheduling center is also relatively high, as shown in Table II. In contrast to the centralized scheduling, the proposed distributed methods allow each user to calculate its own scheduling metric. For GS, such metric is explicitly fed back; for CS, only the orders of these metrics are relevant and no explicitly feedback is necessary. Therefore, the distributed schemes significantly reduce the computational complexity at the relay. It is also noted that Min-UA and ER-UA transmission schemes show different performance-complexity tradeoffs. For the Min-UA transmission, the low implementation complexity is achieved at the cost of insufficiently utilized MuD gain; only when the number of users is large, the distributed scheduling shows distinctive performance improvement. On the other hand, the ER-UA transmission allows the near-optimal distributed scheduling; therefore, it is sufficient to apply the distributed scheduling to effectively harvest the full MuD order.

⁹By using the big O notation, we subsume the computation with respect to the SSA, matrix inversion and etc. We only maintain the key parameter M and some necessary constants (a_1 , a_2 , b_1 and b_2) to highlight the distributed nature our proposed scheme.

TABLE I
CSI OVERHEAD ANALYSIS FOR DIFFERENT SCHEDULING SCHEMES

Schemes	Node	CS		GS	
		Centralized	Distributed	Centralized	Distributed
Min-UA	User	No CSI	Local CSI	No CSI	Local CSI
	Relay	Global CSI	No CSI	Global CSI	2 bits + (2/9) analog feedback per user
ER-UA	User	No CSI	Local CSI	No CSI	Local CSI
	Relay	Global CSI	No CSI	Global CSI	1 analog feedback per user

TABLE II
COMPLEXITY ANALYSIS FOR DIFFERENT SCHEDULING SCHEMES

Schemes	Node	CS		GS	
		Centralized	Distributed	Centralized	Distributed
Min-UA	User	-	$O(1)$	-	$O(1)$
	Relay	$O(M^3)$	-	$O(a_1 M)$	$O(a_2 M)$
ER-UA	User	-	$O(1)$	-	$O(1)$
	Relay	$O(M^3)$	-	$O(b_1 M)$	$O(b_2 M)$

It is noted that $a_1 \gg a_2$ and $b_1 \gg b_2$, since all computation is done by the relay with centralized scheduling. "-" means no computation.

B. Validating Theoretical Derivations for ER-UA Transmission

Fig. 10 and Fig. 11 validate the theoretical derivations of outage probability bounds and the corresponding high SNR approximations for CS and GS with $N = 1$, respectively. It is shown that the derived bounds in Proposition 1, 2, and the relations in (31) and (32) are correct. It is also noted that the developed bounds are loose due to several approximations, e.g., using the minimum eigenvalue to obtain the upper bounds and relaxing the interval of integration for more tractable results, and etc. Fortunately, these bounds are still useful and correct, because they enable the tractable and explicit MuD order in Proposition 3. As verified in the figures, both asymptotic results regarding the UB and LB show the same diversity order, accurately bounding the MuD orders of both the centralized and distributed scheduling schemes with CS and GS, respectively.

VII. CONCLUSION

The distributed cluster-wise scheduling (CS) and group-wise scheduling (GS) have been studied for the MIMO-Y channel with two transmission schemes which have different requirements on the minimum number of user antennas. The RSS has been employed to guide the distributed

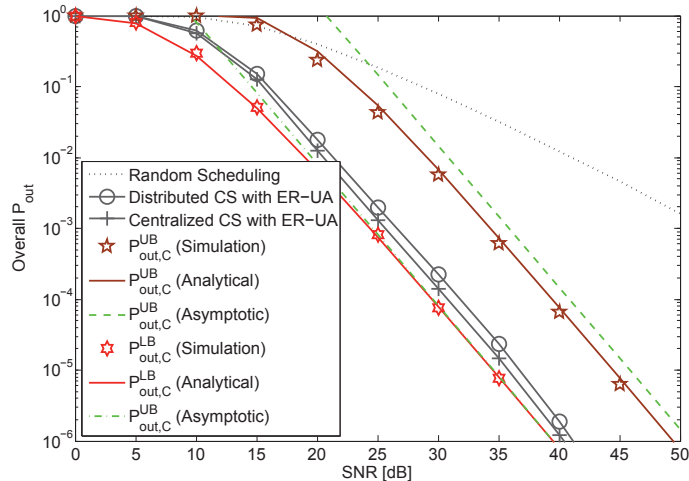


Fig. 11. Overall outage probabilities of the centralized/distributed CS and their bounds with high SNR approximations, where the user configuration is $(2, 3, 4)$ and SNR threshold is $\rho_{th} = 1$.

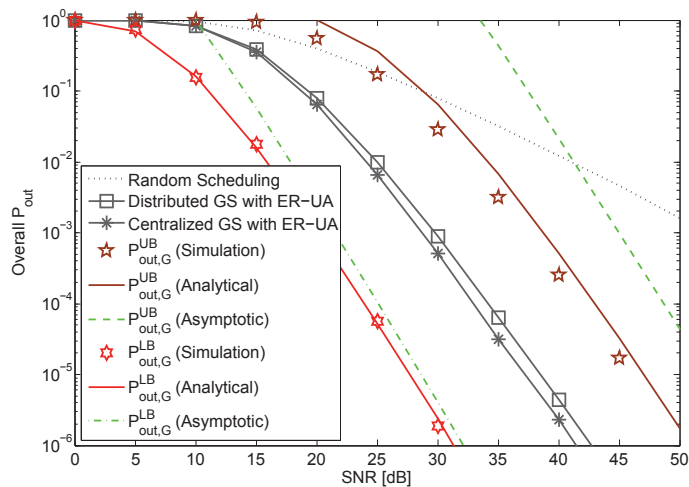


Fig. 12. Overall outage probabilities of the centralized/distributed GS and their bounds with high SNR approximations, where the user group configuration is $M = 3$ and the SNR threshold is $\rho_{th} = 1$.

CS and GS with the Min-UA transmission; and these low-complexity distributed scheduling schemes obtain notable MuD gains when the candidates are abundant. With a simpler yet effective implementation, the RSS-based ER-UA MIMO-Y transmission has been proposed, and the corresponding distributed CS and GS are theoretically proved to achieve the comparable performances as their centralized counterparts. By comparing a variety of scheduling schemes with Min-UA and ER-UA transmissions, the performance-complexity tradeoffs of user scheduling

has been revealed for the MIMO-Y channel. Moreover, DMT analysis with ER-UA transmission shows that the achievable MuD gain is limited by the minimum number of users in the three clusters, which sheds light into the fundamental behavior of MuD in the MIMO-Y channel. Extending the distributed scheduling to the more general multi-way relay channels is a promising future work, while the analysis for the explicit MuD behaviors with the Min-UA transmission is still open. Moreover, it is noted that the proposed scheme is based on a simple system model. Recently, some new MIMO channel modeling methods are reported in [38], [39]. Studying the distributed user scheduling and the optimal beamforming for these new channel models has more practical value and will be of interest for future research.

APPENDIX

APPENDIX I PROOF OF PROPOSITION 1

Proof: For inequality (a1), use Lemma 1 in Appendix VI to obtain $\tilde{\lambda}_{j_k} := \lambda_{\min}(\mathbf{H}_{j_k} \mathbf{H}_{j_k}^H) \leq \alpha_{m,j_k}^2$, $\forall m \in \{\pi(l, k) : l \in \mathcal{L}_k\}$. Therefore, $\tilde{\lambda}_{j_k} \leq \alpha_{j_k}^2 := \min_m \{\alpha_{m,j_k}^2\}$ for $\forall j_k \in [1, M_K]$. By choosing $j_k = j_k^*$, we have

$$\tilde{\lambda}_{j_k^*} \leq \alpha_{j_k^*}^2. \quad (44)$$

On the other hand, note that $j_k^\dagger = \arg \max_{j_k \in [1, M_k]} (\alpha_{j_k}^2)$, i.e., j_k^\dagger is optimal for $\alpha_{j_k}^2$; by using Lemma 2 in Appendix VI, it is easy to obtain

$$\alpha_{j_k^*}^2 \leq \alpha_{j_k^\dagger}^2, \quad k \in [1, 3]. \quad (45)$$

Combining (44) and (45) we have

$$\tilde{\lambda}_{j_k^*} \leq \alpha_{j_k^\dagger}^2, \quad k \in [1, 3]. \quad (46)$$

Based on $J_\lambda = \{\tilde{\lambda}_{j_1^*}, \tilde{\lambda}_{j_2^*}, \tilde{\lambda}_{j_3^*}\}$, we introduce $\zeta_{\min}^{(J_\lambda)} := \min_{k \in [1, 3], l \in \mathcal{L}_k} \left(g(\tilde{\lambda}_{j_k^*}, \tilde{\lambda}_{j_l^*}) \right)$, where $g(x, y) := \frac{xy\text{SNR}}{2x+6(1+\text{SNR}^{-1})}$. It is also noted that $\rho_{\min, CS}^{(J_D)} = \min_{k \in [1, 3], l \in \mathcal{L}_k} \left(g(\alpha_{j_k^\dagger}^2, \alpha_{j_l^\dagger}^2) \right)$. According to (46) and the monotonicity of $g(x, y)$, it is easy to check that

$$\zeta_{\min}^{(J_\lambda)} \leq \rho_{\min, CS}^{(J_D)}. \quad (47)$$

Finally, note that $\tilde{\lambda}_{[n]}^{(J_\lambda)}$ is the n -th largest element of J_λ , then according to Lemma 3 in Appendix VI, we can see that

$$\rho_{\min, CS}^{LB} := g\left(\tilde{\lambda}_{[3]}^{(J_\lambda)}, \tilde{\lambda}_{[2]}^{(J_\lambda)}\right) \leq \zeta_{\min}^{(J_\lambda)}. \quad (48)$$

Combining (48) and (47), the inequality (a1) is proved. Next, according to Lemma 2 in Appendix VI, the inequality (a2) is straightforward by noting that J_C is optimal for $\rho_{min,CS}^{(J)}$. For inequality (a3), it is observed that

$$\rho_{min,CS}^{(J_C)} \leq \rho_{j_2^*, j_1^*} = g\left(\alpha_{1,j_1^*}^2, \alpha_{1,j_2^*}^2\right) \leq g\left(\alpha_{1,j_1^\dagger}^2, \alpha_{1,j_2^\dagger}^2\right), \quad (49)$$

where $\{j_1^*, j_2^*\} \subset J_C$ and the last inequality is based on the monotonicity of $g(x, y)$ and Lemma 2 in Appendix VI, i.e., $\alpha_{1,j_k^*}^2 \leq \alpha_{1,j_k^\dagger}^2$ and j_k^\dagger is defined to be optimal for α_{1,j_k}^2 . Then the proof is finished. \blacksquare

APPENDIX II PROOF OF PROPOSITION 2

Proof: Recall that $\rho_{j_l', j_k'} = g\left(\alpha_{m,j_l'}^2, \alpha_{m,j_k'}^2\right)$ and $\alpha_{j_k'}^2 = \min_{m \in \{I, II, III\}} \left\{ \alpha_{m,j_k'}^2 \right\}$, then according to the monotonicity of $g(x, y)$, it is easy to arrive

$$\rho_{j_l', j_k'} \geq g\left(\alpha_{m,j_l'}^2, \alpha_{m,j_k'}^2\right) \geq g\left(\alpha_{j_l'}^2, \alpha_{j_k'}^2\right), \quad (50)$$

Let us denote $\left(\alpha_{[n]}^{(J')}\right)^2$ and $\tilde{\lambda}_{[n]}^{(J')}$ as the n -th largest elements of $\left\{ \alpha_{j_1'}^2, \alpha_{j_2'}^2, \alpha_{j_3'}^2 \right\}$ and $\left\{ \tilde{\lambda}_{j_1'}, \tilde{\lambda}_{j_2'}, \tilde{\lambda}_{j_3'} \right\}$, where $\tilde{\lambda}_{j_k} := \lambda_{min}(\mathbf{H}_{j_k} \mathbf{H}_{j_k}^H)$. Then we can construct a lower bound of $\rho_{min,GS}^{(J')} = \min_{k \in [1,3], l \in \mathcal{L}_k} \left(\rho_{j_l', j_k'} \right)$ as

$$\begin{aligned} \rho_{min,GS}^{(J')} &\geq \min_{k \in [1,3], l \in \mathcal{L}_k} \left(g\left(\alpha_{j_l'}^2, \alpha_{j_k'}^2\right) \right) \\ &\geq g\left(\left(\alpha_{[3]}^{(J')}\right)^2, \left(\alpha_{[2]}^{(J')}\right)^2\right) := \gamma_{min}^{(J')} \\ &\geq g\left(\tilde{\lambda}_{[3]}^{(J')}, \tilde{\lambda}_{[2]}^{(J')}\right) := \zeta_{min}^{(J')}, \end{aligned} \quad (51)$$

where the first inequality is based on (50), the second inequality is based on Lemma 3 in Appendix VI and the third inequality is based on Lemma 1 in Appendix VI and the monotonicity of $g(x, y)$. According to (51), it is easy to show that

$$\rho_{min,GS}^{(J')} \geq \gamma_{min}^{(J')} \geq \zeta_{min}^{(J')}, \quad \forall J' \in \mathcal{J}', \quad (52)$$

then we proceed to obtain the following inequalities

$$\rho_{min,GS}^{(J'_D)} \geq \gamma_{min}^{(J'_D)} \geq \gamma_{min}^{(J_\zeta)} \geq \zeta_{min}^{(J_\zeta)} := \rho_{min,GS}^{LB}, \quad (53)$$

where J_ζ is defined as $J_\zeta = \arg \max_{J' \in \mathcal{J}'} \left\{ \zeta_{min}^{(J')} \right\}$. i.e., $\zeta_{min}^{(J_\zeta)} = \max_{J' \in \mathcal{J}'} \left\{ g\left(\tilde{\lambda}_{[3]}^{(J')}, \tilde{\lambda}_{[2]}^{(J')}\right) \right\} = \rho_{min,GS}^{LB}$. Here, the first and the third inequalities are based on the basic relations in (52), and the second inequality is based on the optimality of J'_D for $\left\{ \gamma_{min}^{(J')} \right\}$ and Lemma 2 in Appendix VI. It is noted that the inequalities in (53) have been used to prove the inequality (b1) in (30). Then,

the inequality (b2) is based on the fact that J'_C is optimal for $\rho_{min}^{(J')}$ and Lemma 2 in Appendix VI, where $J' \in \mathcal{J}'$. For the inequality (b3), it is noted that

$$\rho_{min,GS}^{(J'_C)} \leq \rho_{j_2'^*, j_1'^*} = g\left(\alpha_{1,j_1'^*}^2, \alpha_{1,j_2'^*}^2\right) \leq g\left(\alpha_{1,j_1^\dagger}^2, \alpha_{1,j_2^\dagger}^2\right)$$

where $\{j_1'^*, j_2'^*\} \subset J'_C$ and the last inequality is based on the monotonicity of $g(x, y)$ and Lemma 2 in Appendix VI, i.e., $\alpha_{1,j_k'^*}^2 \leq \alpha_{1,j_k^\dagger}^2$ and j_k^\dagger is defined to be optimal for α_{1,j_k}^2 . ■

APPENDIX III DERIVATIONS FOR $P_{out,CS(GS)}^{LB}$, $P_{out,CS}^{UB}$ AND $P_{out,GS}^{UB}$

As the preliminary, the relevant distributions of the key random variables (RVs) are given. First, according to Lemma 3 in Appendix VI, it is known that α_{m,j_k}^2 is exponentially distributed with the probability density function (PDF) as $f_{\alpha_{m,j_k}^2}(x) = e^{-x}$, therefore, the order statistic [40] is applied to these i.i.d. RVs, and we obtain the PDF of $\alpha_{m,j_k^\dagger}^2$ as $f_{\alpha_{m,j_k^\dagger}^2}(x) = M_k (1 - e^{-x})^{M_k-1} e^{-x}$. According to [41], $\tilde{\lambda}_{j_k} = \lambda_{min}(\mathbf{H}_{j_k} \mathbf{H}_{j_k}^H)$ is also exponentially distributed as $f_{\alpha_{m,j_k}^2}(x) = e^{-3x}$, therefore, the PDF of $\tilde{\lambda}_{j_k^*}$ is given by $f_{\tilde{\lambda}_{j_k^*}}(x) = M_k (1 - e^{-3x})^{M_k-1} e^{-3x}$. Then, we continue the derivations for $P_{out,CS(GS)}^{LB}$, $P_{out,CS}^{UB}$ and $P_{out,GS}^{UB}$.

$P_{out,CS(GS)}^{LB}$: Let us first define $X = \alpha_{1,j_1^\dagger}^2$ and $Y = \alpha_{1,j_2^\dagger}^2$, then we can express the LB of outage probability as $P_{out,CS}^{LB}(\rho_{th}) = \int_0^\infty f_Y(y) \left(\int_0^{a+\frac{b}{y}} f_X(x) dx \right) dy$, where $a(\rho_{th}) = \frac{2\rho_{th}}{\text{SNR}}$ and $b(\rho_{th}) = \frac{6\rho_{th}(\text{SNR}+1)}{\text{SNR}^2}$. After some straightforward calculations, $P_{out,CS}^{LB}(\rho_{th})$ is given in (33).

$P_{out,CS}^{UB}$: With a slight abuse of notations, let us define $X = \tilde{\lambda}_{j_1^*}$, $Y = \tilde{\lambda}_{j_2^*}$ and $Z = \tilde{\lambda}_{j_3^*}$, and introduce the ordered set $\Theta = \{\Theta_i\}_{i=1}^6$ to collect all the permutations among $\{X, Y, Z\}$, where $\Theta_i = \{\theta_{i,n}\}_{n=1}^3$, e.g., $\Theta_1 = \{\theta_{1,1}, \theta_{1,2}, \theta_{1,3}\} = \{X, Y, Z\}$, $\Theta_2 = \{\theta_{2,1}, \theta_{2,2}, \theta_{2,3}\} = \{X, Z, Y\}$ and so on. We also associate Θ_i with an event as O_i , which orders the elements of Θ_i , e.g., $\Theta_1 = \{X, Y, Z\} \leftrightarrow O_1 = \{X \geq Y \geq Z\}$. Then we divide the whole integral region into six subregions to facilitate the calculation, where each subregion is associated with O_i , $i \in [1, 6]$. Based on such division, $P_{out,CS}^{UB}(\rho_{th})$ is re-expressed as

$$P_{out}^{UB}(\rho_{th}) = \sum_{i=1}^6 \Pr\{E_i(\rho_{th})\}, \quad (54)$$

where $E_i(\rho_{th}) = \{g(\theta_{i,[3]} \theta_{i,[2]}) \leq \rho_{th}, O_i\}$, $\theta_{i,[n]}$ is the n -th largest element of Θ_i . Without loss of generality, let us focus on the probability of $E_1(\rho_{th})$, given by $\Pr\{E_1(\rho_{th})\} = \sum_{t=1}^3 \int \int \int_{D_{1,t}} f(x, y, z) dx dy dz = \sum_{t=1}^3 I_{1,t}$, where $f(x, y, z) = f_X(x) f_Y(y) f_Z(z)$ due to independence, and the integral region of $I_{1,t}$ is $D_{1,t} = \{(x, y, z) | x \in \mathcal{X}_{1,t}, y \in \mathcal{Y}_{1,t}, z \in \mathcal{Z}_{1,t}\}$, i.e., $\int_{\mathcal{X}_{1,n}} \int_{\mathcal{Y}_{1,n}} \int_{\mathcal{Z}_{1,n}}$. Then $I_{1,1} = \int_0^\mu \int_0^x \int_0^y f(x, y, z) dx dy dz$ and $I_{1,2} = \int_\mu^\infty \int_0^\mu \int_0^y f(x, y, z) dx dy dz$

are obtained after some calculations as

$$I_{1,1} = \frac{M_2 M_3 (1 - e^{-3\mu})^{M_\Sigma}}{(M_1 + M_2) M_\Sigma}, \quad (55)$$

$$I_{1,2} = \frac{M_2 (1 - e^{-3\mu})^{M_1 + M_2} [1 - (1 - e^{-3\mu})^{M_3}]}{M_1 + M_2}, \quad (56)$$

where $\mu = \frac{1}{2} (a + \sqrt{a^2 + 4b})$ is the positive root of the quadratic equation $y^2 = ay + b$, $a(\rho_{th}) = \frac{2\rho_{th}}{\text{SNR}}$, $b(\rho_{th}) = \frac{6\rho_{th}(\text{SNR}+1)}{\text{SNR}^2}$ and $M_\Sigma = M_1 + M_2 + M_3$. It is note that $I_{1,3} = \int_{\mu}^{\infty} \int_{\mu}^x \int_0^{a+\frac{b}{y}} f(x, y, z) dx dy dz$ is not easy to calculate with tractable results, thus the following approximations is used as $I_{1,3} < I'_{1,3} = \int_{\mu}^{\infty} \int_{\mu}^{\infty} \int_0^{a+\frac{b}{y}} f(x, y, z) dx dy dz$, where the integral region regarding variable y has been enlarged. After some calculations, the result of $I'_{1,3}$ is given by

$$I'_{1,3} = \left[3M_2 \sum_{p=0}^{M_2-1} \sum_{q=0}^{M_1} (-1)^q C_p^{M_2-1} C_q^{M_1} e^{-3qa} \int_{\mu}^{\infty} e^{-3((p+1)y - qb\frac{1}{y})} dy \right] [1 - (1 - e^{-3\mu})^{M_3}], \quad (57)$$

then $\Pr \{E_1(\rho_{th})\} \approx I_{1,1} + I_{1,2} + I'_{1,3}$ is obtained. It is also noted that the permutation of $\{X, Y, Z\}$ and the user configuration $\{M_1, M_3, M_3\}$ have a fixed matching pattern in $E_i(\rho_{th})$; therefore, we can modify the results of $\Pr \{E_1(\rho_{th})\}$ in (55), (56) and (57) to get $\Pr \{E_i(\rho_{th})\}$, $i \in [2, 6]$, and finally arrive at the result in (34).

$P_{out,GS}^{UB}$: Applying the order statistics of i.i.d. RVs, $P_{out,GS}^{UB}(\rho_{th})$ is expanded as

$$P_{out,GS}^{UB}(\rho_{th}) = \Pr(\underline{\rho}_{min,GS} \leq \rho_{th}) = \left[\Pr\left(\zeta_{min}^{(J')} \leq \rho_{th}\right) \right]^M, \quad (58)$$

where $\zeta_{min}^{(J')}$ is defined in (51). It is also noted that the approximation of $\Pr\left(\zeta_{min}^{(J')} \leq \rho_{th}\right)$ can be easily obtained by substituting $M_1 = M_2 = M_3 = 1$ into (55), (56), (57), and after some calculations, we have the result in (35).

APPENDIX V PROOF OF PROPOSITION 3

Proof: Let us focus on the CS scenario first, the LB of $P_{out,CS}(\text{SNR})$ is given by

$$\begin{aligned} P_{out,CS}(\text{SNR}) &\geq \Pr(R_{CS}^{UB} \leq R_{th}(\text{SNR})) \\ &= \Pr\left(\bar{\rho}_{min,CS} \leq (1 + \text{SNR})^{\frac{\tau}{3}} - 1\right) \\ &= P_{out,CS}^{LB}(\text{SNR}), \end{aligned} \quad (59)$$

where $R_{CS}^{UB} = 3 \log_2(1 + \bar{\rho}_{min,CS})$ is the UB of R . Then, according to the high SNR analysis in (36) and Lemma 4 in Appendix VI, it is easy to check that

$$P_{out,CS}^{LB} \doteq \text{SNR}^{-d_{CS}^{UB}(1-\frac{\tau}{3})}. \quad (60)$$

One the other hand, the UB of $P_{out,CS}(\text{SNR})$ is given by

$$\begin{aligned}
P_{out,CS}(\text{SNR}) &\leq \Pr(R_{CS}^{LB} \leq R_{th}(\text{SNR})) \\
&= \Pr\left(\rho_{min,CS} \leq (1 + \text{SNR})^{\frac{r}{3}} - 1\right) \\
&= P_{out,CS}^{UB}(\text{SNR}),
\end{aligned} \tag{61}$$

where $R_{CS}^{LB} = 3 \log_2(1 + \rho_{min,CS})$ is the lower bound of R . Based on (37) and Lemma 4 in Appendix VI, it is shown that

$$P_{out,CS}^{UB}(\text{SNR}) \doteq \text{SNR}^{-d_{CS}^{LB}(1-\frac{r}{3})}. \tag{62}$$

Noting $d_{CS}^{UB} = d_{CS}^{LB} = \min\{M_1, M_2, M_3\}$, the DMT in (42) for CS scenario is obtained by combining (59) to (62). The DMT analysis for the GS scenario follows the similar procedures as the CS scenario, and we omit this part for limited space. The proof is then finished. ■

APPENDIX IV DERIVATIONS FOR THE HIGH SNR APPROXIMATIONS

The high SNR approximations aim to facilitate the extraction of the MuD gain. Although the results in (34) and (35) are easy to be evaluated with software, they involve integral of exponential functions and are not easy to be further analyzed. To this end, some approximations are applied before the high SNR analysis. Specifically, $I'_{1,3}$ in (57) is further approximated as $I'_{1,3} < I''_{1,3} = \int_0^\infty \int_0^\infty \int_0^{\alpha+\frac{b}{y}} f(x, y, z) dx dy dz$, where the integral intervals of x and y have been enlarged from $x, y \in [\mu, \infty)$ to $x, y \in [0, \infty)$. The rational of this approximation is that when SNR is high, the condition $\mu \rightarrow 0$ holds, and such approximation will not influence the asymptotic behaviors that are relevant to the MuD gain. Then the result of $I''_{1,3}$ is given by

$$\begin{aligned}
I''_{1,3} &= 2M_2 \sum_{q=0}^{M_2-1} \left[\frac{(-1)^q \binom{M_2-1}{q}}{2(q+1)} + 3 \sum_{p=1}^{M_1} \binom{M_2-1}{q} \binom{M_1}{p} (-1)^{q+p} e^{-3pa} \sqrt{\frac{pb}{(q+1)}} K_1\left(6\sqrt{p(q+1)b}\right) \right] \\
&\quad \times \left[1 - (1 - e^{-3\mu})^{M_3} \right].
\end{aligned} \tag{63}$$

By using $I''_{1,3}$, $\Pr\{E_1(\rho_{th})\}$ is further approximated as $\Pr\{E_1(\rho_{th})\} < \bar{\Pr}\{E_1(\rho_{th})\} = I_{1,1} + I_{1,2} + I''_{1,3}$. Following the same lines of the derivations of $P_{out,CS}^{UB}$, we have the approximation $P_{out,CS}^{UB} < \bar{P}_{out,CS}^{UB} = \sum_{i=1}^6 \bar{\Pr}\{E_i(\rho_{th})\}$. It is noted that $\bar{P}_{out,CS}^{UB}$ can be obtained by replacing the second item of summation in (34) with a slight modification of $I''_{1,3}$, i.e., changing M_k into

$M_{i,k}$, $k \in [1, 3]$, which is given by

$$\begin{aligned} \bar{P}_{out,CS}^{UB}(\rho_{th}) &\approx \sum_{i=1}^6 \left(\frac{M_{i,2}M_{i,3}(1-e^{-3\mu})^{M_\Sigma} + M_{i,2}M_\Sigma(1-e^{-3\mu})^{M_{i,1}+M_{i,2}} \left[1 - (1-e^{-3\mu})^{M_{i,3}}\right]}{(M_{i,1} + M_{i,2})M_\Sigma} \right. \\ &\quad \left. + 2M_{i,2} \sum_{q=0}^{M_{i,2}-1} \left[\frac{(-1)^q \binom{M_{i,2}-1}{q}}{2(q+1)} + 3 \sum_{p=1}^{M_{i,1}} \binom{M_{i,2}-1}{q} \binom{M_{i,1}}{p} (-1)^{q+p} e^{-3pa} \sqrt{\frac{pb}{(q+1)}} K_1\left(6\sqrt{p(q+1)b}\right) \right] \right. \\ &\quad \left. \times \left[1 - (1-e^{-3\mu})^{M_{i,3}}\right] \right). \end{aligned} \quad (64)$$

On the other hand, by substituting $M_1 = M_2 = M_3 = 1$ in $\bar{P}_{out,CS}^{UB}$ and following the derivation of $P_{out,GS}^{UB}$, we have $P_{out,GS}^{UB} < \bar{P}_{out,GS}^{UB}$, and $\bar{P}_{out,GS}^{UB}$ is obtained by replacing the third item in (35) with $6e^{-3\mu} \left(1 - e^{-3a} 6\sqrt{b} K_1(6\sqrt{b})\right)$, which is given by

$$P_{out,GS}^{UB}(\rho_{th}) \approx \left[3(1-e^{-3\mu})^2 - 2(1-e^{-3\mu})^3 + 6e^{-3\mu} \left(1 - e^{-3a} 6\sqrt{b} K_1(6\sqrt{b})\right) \right]^M. \quad (65)$$

Then, $P_{out,C(G)}^{LB}$ and $\bar{P}_{out,CS(G)}^{UB}$ are actually used to continue the high SNR analysis.

For the high SNR analysis, we first approximate $b = \frac{6\rho_{th}(\text{SNR}+1)}{\text{SNR}^2} \approx \frac{6\rho_{th}}{\text{SNR}} = 3a$ and $\mu \approx \frac{1}{2}(a + \sqrt{a^2 + 12a})$, consequently, $P_{out,C(G)}^{LB}$ and $\bar{P}_{out,C(G)}^{UB}$ can be defined as functions of a . Then the power series of the exponential function e^x and the modified Bessel function $K_1(x)$ [42] are used to express $P_{out,C(G)}^{LB}$ and $\bar{P}_{out,C(G)}^{UB}$ with the polynomial forms regarding a . By finding the first nonzero derivative orders of these polynomials and discarding the higher order infinitesimal terms when $a \rightarrow 0$, the key results are obtained and shown in (36)-(39).

APPENDIX VI LEMMAS

Lemma 1. The equivalent channel coefficient $\alpha_{m,j_k} = \|\mathbf{H}_{j_k}^{-1} \mathbf{e}_m\|^{-1}$ with $\forall j_k \in [1, M_k]$ and $\forall m \in \{\pi(l, k) : l \in \mathcal{L}_k\}$ is lower bounded by the minimum eigenvalue of $\mathbf{H}_{j_k} \mathbf{H}_{j_k}^H$, i.e., $\tilde{\lambda}_{j_k} := \lambda_{\min}(\mathbf{H}_{j_k} \mathbf{H}_{j_k}^H) \leq \alpha_{m,j_k}$

Proof: Note that $\|\mathbf{e}_m\| = 1$, then according to Rayleigh-Ritz theorem [36] the lemma can be proved. ■

Lemma 2. For two objective functions η_A and η_B with respect to the selected users $J = \{j_1, j_2, j_3\}$, the optimal selections are defined as $J_A = \arg \max_{J \in \mathcal{J}} \left(\eta_A^{(J)}\right)$ and $J_B = \arg \max_{J \in \mathcal{J}} \left(\eta_B^{(J)}\right)$ respectively, then $\eta_A^{(J_B)} \leq \eta_A^{(J_A)}$ and $\eta_B^{(J_A)} \leq \eta_B^{(J_B)}$.

Proof: Based on its definition, J_A maximizes $\eta_A^{(J)}$ over $J \in \mathcal{J}$, therefore no any other $J' \in \mathcal{J}$, $J' \neq J_A$ can achieve larger $\eta_A^{(J')}$ than $\eta_A^{(J_A)}$. Let $J' = J_B$, $\eta_A^{(J_B)} \leq \eta_A^{(J_A)}$ is proved. For the same reason $\eta_B^{(J_A)} \leq \eta_B^{(J_B)}$ can be proved. ■

Lemma 3. For a set $\{x_1, x_2, x_3\}$, $x_i > 0$, $i = 1, 2, 3$, define an ordered set \mathcal{X} containing all 2-element permutations of $\{x_1, x_2, x_3\}$, i.e., $\mathcal{X} = \{(x_1, x_2) (x_2, x_1) \dots (x_2, x_3) (x_3, x_2)\}$, and let $x_{[n]}$ as the n -th largest element of $\{x_1, x_2, x_3\}$. Then the following inequality holds

$$g(x_{[3]}, x_{[2]}) \leq \min_{(\tilde{x}_1, \tilde{x}_2) \in \mathcal{X}} (g(\tilde{x}_1, \tilde{x}_2)),$$

where $g(\tilde{x}_1, \tilde{x}_2) := \frac{\tilde{x}_1 \tilde{x}_2 \text{SNR}}{2\tilde{x}_2 + 6(1 + \text{SNR}^{-1})}$ is defined over \mathcal{X} and monotonically increases with \tilde{x}_1 and \tilde{x}_2 .

Proof: Note that $g(\tilde{x}_1, \tilde{x}_2)$ monotonically increases with \tilde{x}_1 and \tilde{x}_2 , it is easy to check that $\min_{(\tilde{x}_1, \tilde{x}_2) \in \mathcal{X}} (g(\tilde{x}_1, \tilde{x}_2)) = \min(g(x_{[3]}, x_{[2]}), g(x_{[2]}, x_{[3]})) = g(x_{[3]}, x_{[2]})$, and the proof is finished. ■

Lemma 4. Given $\mathbf{e}_m^{[n]}$, a reference direction from the orthogonal basis \mathbf{E} of the RSS, and the channel matrix \mathbf{H}_{j_k} with i.i.d. $\mathcal{CN}(0, 1)$ entries, the equivalent channel gain $(\alpha_{m,j_k}^{[n]})^2 = \left\| \mathbf{H}_{j_k}^{-1} \mathbf{e}_m^{[n]} \right\|^{-2}$ of the n -th data stream within the link $\mathcal{S}_{j_k} \rightarrow \mathcal{R}$ is exponentially distributed as $f_{(\alpha_{m,j_k}^{[n]})^2}(x) = e^{-x}$.

Proof: Firstly, it is noted that $\mathbf{e}_m^{[n]} = \mathbf{E} \mathbf{a}_{m'}$, where $\mathbf{a}_{m'} \in \mathbb{C}^{3N \times 1}$ has all zero elements except the m' -th element that equals to one. It is noted that $m' = (m-1)N + n$, $m \in \{1, 2, 3\}$ and $n \in [1, N]$. Then $(\alpha_{m,j_k}^{[n]})^2$ is re-expressed as

$$(\alpha_{m,j_k}^{[n]})^2 = \left\| \mathbf{H}_k^{-1} \mathbf{E} \mathbf{a}_{m'} \right\|^{-2} = \left[\left(\tilde{\mathbf{H}}_{j_k} \tilde{\mathbf{H}}_{j_k}^H \right)^{-1} \right]_{m',m'}^{-1}, \quad (66)$$

Note that $\mathbf{H}_{j_k} \mathbf{H}_{j_k}^H$ and $\tilde{\mathbf{H}}_{j_k} \tilde{\mathbf{H}}_{j_k}^H = \mathbf{E} \mathbf{H}_{j_k} \mathbf{H}_{j_k}^H \mathbf{E}^H$ have the same statistic properties, because of the independence between \mathbf{E} and \mathbf{H}_{j_k} , and the unitarily invariant of the central Wishart matrix [43]. According to [44], we know $\left[\left(\mathbf{H}_{j_k} \mathbf{H}_{j_k}^H \right)^{-1} \right]_{m',m'}^{-1}$ is exponentially distributed with a PDF $f(x) = e^{-x}$, so is $(\alpha_{m,j_k}^{[n]})^2$ as defined in (66), and the proof is finished. ■

Lemma 5. $\left(\frac{c}{\text{SNR}} \right)^d \ln \left(\frac{\text{SNR}}{c} \right) \doteq \text{SNR}^{-d}$

Proof: Using the l'Hospital's rule, it is easy to check that $\left(\frac{c}{\text{SNR}} \right)^d = o \left(\left(\frac{c}{\text{SNR}} \right)^d \ln \left(\frac{\text{SNR}}{c} \right) \right)$

and $\left(\frac{c}{\text{SNR}}\right)^d \ln\left(\frac{\text{SNR}}{c}\right) = o\left(\left(\frac{c}{\text{SNR}}\right)^{d-\epsilon}\right)$ when $\text{SNR} \rightarrow \infty$ with $\forall \epsilon > 0$, and the inequality

$$\begin{aligned} c_1 \lim_{\text{SNR} \rightarrow \infty} \left(\frac{c}{\text{SNR}}\right)^d &< \lim_{\text{SNR} \rightarrow \infty} \left(\frac{c}{\text{SNR}}\right)^d \ln\left(\frac{\text{SNR}}{c}\right) \\ &< c_2 \lim_{\text{SNR} \rightarrow \infty} \left(\frac{c}{\text{SNR}}\right)^{d-\epsilon}, \end{aligned} \quad (67)$$

holds for some c_1 and c_2 . Let $\epsilon \rightarrow 0$ in (67), then $\left(\frac{c}{\text{SNR}}\right)^{d-\epsilon} \rightarrow \left(\frac{c}{\text{SNR}}\right)^d$ and $\left(\frac{c}{\text{SNR}}\right)^d \ln\left(\frac{\text{SNR}}{c}\right) \doteq \text{SNR}^{-d}$, and the proof is finished. ■

REFERENCES

- [1] D. Gunduz, A. Yener, A. Goldsmith, and H. Poor, "The multiway relay channel," *IEEE Trans. Inf. Theory*, vol. 59, pp. 51–63, Jan. 2013.
- [2] A. Chaaban and A. Sezgin, "On channel inseparability and the dof region of MIMO multi-way relay channels," pp. 1–7, 2014. [Online]. Available: <http://arxiv.org/abs/1412.0914v1>
- [3] L. Ong, S. J. Johnson, and C. M. Kellett, "The capacity region of multiway relay channels over finite fields with full data exchange," *IEEE Trans. Inf. Theory*, vol. 57, pp. 3016–3031, May 2011.
- [4] T. Cui, J. Kliewer, and T. Ho, "Communication protocols for N-way all-cast relay networks," *IEEE Trans. Commun.*, vol. 60, pp. 3239–3251, Nov. 2012.
- [5] H. Degenhardt, Y. Rong, and A. Klein, "Non-regenerative multi-way relaying: Combining the gains of network coding and joint processing," *IEEE Trans. Wireless Commun.*, vol. 12, pp. 5692–5703, Nov. 2013.
- [6] S. Katti, S. Gollakota, and D. Katabi, "Embracing wireless interference: Analog network coding," in *Proc. ACM SIGCOMM*, Kyoto, Japan, Aug. 2007, pp. 397–408.
- [7] S. Zhang, S. Liew, and P. Lam, "Hot topic: physical-layer network coding," in *Proc. 12th ACM MobiCom*, Los Angeles, CA, USA, Sept. 2006, pp. 358–365.
- [8] L. Song, Y. Li, A. Huang, B. Jiao, and A. V. Vasilakos, "Differential modulation for bidirectional relaying with analog network coding," *IEEE Trans. Signal Process.*, vol. 58, pp. 3933–3938, Jun. 2010.
- [9] A. S. Avestimehr, A. Sezgin, and D. N. Tse, "Capacity of the two-way relay channel within a constant gap," *Eur. Trans. Telecommun.*, vol. 21, no. 4, pp. 363–374, Apr. 2010.
- [10] A. Sezgin, A. S. Avestimehr, M. A. Khajehnejad, and B. Hassibi, "Divide-and-conquer: approaching the capacity of the two-pair bidirectional gaussian relay network," *IEEE Trans. Inf. Theory*, vol. 58, pp. 2434–2454, Apr. 2012.
- [11] N. Lee, J. Lim, and J. Chun, "Degrees of freedom of the MIMO Y channel: signal space alignment for network coding," *IEEE Trans. Inf. Theory*, vol. 56, pp. 3332–3342, July 2010.
- [12] V. Cadambe and S. Jafar, "Interference alignment and degrees of freedom of the K user interference channel," *IEEE Trans. Inf. Theory*, vol. 54, pp. 3425–3441, Aug. 2008.
- [13] K. Lee, N. Lee, and I. Lee, "Achievable degrees of freedom on K-user Y channels," *IEEE Trans. Wireless Commun.*, vol. 11, pp. 1210–1219, March 2012.
- [14] A. Chaaban, A. Sezgin, and A. S. Avestimehr, "Approximate sum-capacity of the Y-channel," *IEEE Trans. Inf. Theory*, vol. 59, pp. 5723–5740, Sept. 2013.
- [15] A. Chaaban and A. Sezgin, "The approximate capacity region of the gaussian Y-channel via the deterministic approach," *IEEE Trans. Inf. Theory*, Early Access Online, Dec. 2014.

- [16] W. Long, T. Lv, and H. Gao, "Asymmetric signal space alignment for Y channel with single-antenna users," in *Proc. IEEE ICC*, Budapest, Hungary, June 2013, pp. 3427–3431.
- [17] B. Yuan, X. Liao, F. Gao, and X. Luo, "Achievable degrees of freedom of the four-user MIMO Y channel," *IEEE Commun. Lett.*, vol. 18, pp. 6–9, Jan. 2014.
- [18] N. Wang, Z. Ding, T. Dai, and A. Vasilakos, "On generalized MIMO Y channels: precoding design, mapping and diversity gain," *IEEE Trans. Veh. Technol.*, vol. 60, pp. 3525–3532, Sept. 2011.
- [19] Z. Zhou and B. Vucetic, "An iterative beamforming optimization algorithm for generalized MIMO Y channels," in *Proc. IEEE ICC*, Ottawa, Canada, June. 2012, pp. 1–5.
- [20] K. Teav, Z. Zhou, and B. Vucetic, "Throughput optimization for MIMO Y channels with physical network coding and adaptive modulation," in *Proc. IEEE VTC*, Yokohama, Japan, May 2012, pp. 1–5.
- [21] D. Tse and P. Viswanath, *Fundamentals of Wireless Communication*. Cambridge, U.K: Cambridge University Press, 2005.
- [22] D. Gesbert and M.-S. Alouini, "How much feedback is multi-user diversity really worth?" in *Proc. IEEE ICC*, 2004, pp. 234–238.
- [23] T. Yoo and A. Goldsmith, "On the optimality of multiantenna broadcast scheduling using zero-forcing beamforming," *IEEE J. Sel. Areas Commun.*, vol. 24, pp. 528–541, March 2006.
- [24] H. J. Yang, W.-Y. Shin, B. C. Jung, and A. Paulraj, "Opportunistic interference alignment for MIMO interfering multiple-access channels," *IEEE Trans. Wireless Commun.*, vol. 12, pp. 2180–2192, May 2013.
- [25] J. H. Lee and W. Choi, "On the achievable DoF and user scaling law of opportunistic interference alignment in 3-transmitter MIMO interference channels," *IEEE Trans. Wireless Commun.*, vol. 12, pp. 2743–2753, June 2013.
- [26] P. K. Upadhyay and S. Prakriya, "Outage-optimal opportunistic scheduling with analog network coding in multiuser two-way relay networks," *EURASIP J. Wireless Commun. Netw.*, vol. 2011, pp. 1–12, 2011.
- [27] Y. Jeon, Y.-T. Kim, M. Park, and I. Lee, "Opportunistic scheduling for multi-user two-way relay systems with physical network coding," *IEEE Trans. Wireless Commun.*, vol. 11, pp. 1290–1294, Apr. 2012.
- [28] J. Joung and A. Sayed, "User selection methods for multiuser two-way relay communications using space division multiple access," *IEEE Trans. Wireless Commun.*, vol. 9, pp. 2130–2136, July 2010.
- [29] F. Wang, "Wireless MIMO switching: network-coded MMSE relaying and user group selection," *Trans. Emerging Telecommun. Tech.*, pp. 1–8, 2012. [Online]. Available: <http://dx.doi.org/10.1002/ett.2585>
- [30] Y.-U. Jang and Y. H. Lee, "Performance analysis of user selection for multiuser two-way amplify-and-forward relay," *IEEE Commun. Lett.*, vol. 14, pp. 1086–1088, Nov. 2010.
- [31] X. Zhang, M. Peng, Z. Ding, and W. Wang, "Multi-user scheduling for network coded two-way relay channel in cellular systems," *IEEE Trans. Wireless Commun.*, vol. 11, pp. 2542–2551, July 2012.
- [32] H. Gao, C. Yuen, H. A. Suraweera, and T. Lv, "Multiuser diversity for MIMO-Y channel: Max-min selection and diversity analysis," in *Proc. IEEE ICC*, Budapest, Hungary, June 2013, pp. 4379–4384.
- [33] H. Gao, Y. Ren, C. Yuen, and T. Lv, "Distributed scheduling achieves the optimal multiuser diversity gain for MIMO-Y channel," in *Proc. IEEE GLOBECOM Workshop on Emerging Technologies for LTE-Advanced and Beyond-4G*, Atlanta, GA, Dec. 2013, pp. 7–12.
- [34] L. Zheng and D. Tse, "Diversity and multiplexing: A fundamental tradeoff in multiple-antenna channels," *IEEE Trans. Inf. Theory*, vol. 49, pp. 1073–1096, May 2003.
- [35] Z. Ding, T. Wang, M. Peng, W. Wang, and K. Leung, "On the design of network coding for multiple two-way relaying channels," *IEEE Trans. Wireless Commun.*, vol. 10, pp. 1820–1832, June 2011.

- [36] G. H. Golub and C. F. Van Loan, *Matrix computations*. Johns Hopkins University Press, 2012.
- [37] I. Gradshteyn and I. Ryzhik, *Table of Integrals, Series, and Products, 7th ed.* New York: Academic, 2005.
- [38] X. Cheng, C.-X. Wang, D. I. Laurenson, S. Salous, and A. V. Vasilakos, "An adaptive geometry-based stochastic model for non-isotropic MIMO mobile-to-mobile channels," *IEEE Trans. Wireless Commun.*, vol. 8, pp. 4824–4835, Sep. 2009.
- [39] —, "New deterministic and stochastic simulation models for non-isotropic scattering mobile-to-mobile rayleigh fading channels," *Wireless Commun. and Mobile Computing*, vol. 11, no. 7, pp. 829–842, Jul. 2011.
- [40] H. A. David and H. Nagaraja, *Order Statistics*. Wiley, 2004.
- [41] A. Edelman, *Eigenvalues and condition numbers of random matrices*. Ph.D. dissertation, Mass. Inst. Technol. (MIT), Cambridge, Boston, USA, May 1989.
- [42] G. I.S. and R. I.M., *Table of integrals, series, and products*. Access Online via Elsevier, 2007.
- [43] A. M. Tulino and S. Verdú, *Random matrix theory and wireless communications*. Now Publishers, 2004, vol. 1.
- [44] D. Gore, R. W. Heath Jr., and A. Paulraj, "On performance of the zero forcing receiver in presence of transmit correlation," in *Proc. IEEE ISIT*, Palais de Beaulieu, Lausanne, Switzerland, 2002, p. 159.